

Time-series Luminance Distribution Maps:

implementation of annual daylight simulation methods for
occupant visual comfort analysis

Alireza Hashemloo

A thesis

submitted in partial fulfillment of the
requirements for the degree of

Master of Science in Architecture

University of Washington

2016

Committee:

Mehlika Inanici

Christopher Meek

Program Authorized to Offer Degree:

Architecture

© Copyright 2016
Alireza Hashemloo

University of Washington

Abstract

Time-series Luminance Distribution Maps: implementation of annual daylight simulation methods for occupant visual comfort analysis

Alireza Hashemloo

Chair of the Supervisory Committee:

Associate Professor Mehlika Inanici

Department of Architecture

This thesis investigates the existing annual climate-based daylight simulation methodologies for providing time-series luminance distribution data that can be utilized for occupant visual comfort analysis. The motivation is stemmed from an imminent change in lighting research and practice that incorporates more luminance based simulation and metrics, as opposed to the historical use of illuminance based studies. Luminance based metrics provide better understanding of human visual experience, and allows us to design and study occupant centric luminous environments. An implementation workflow for the most advanced annual climate-based daylight simulation methodologies (The Three-phase and Five-phase daylighting simulation methods) based on the existing literature is provided as an explanatory guideline for non-developer designers and daylight practitioners. The simulation workflow is demonstrated using an office space in downtown Seattle. Each methodology's capability to simulate the real-world complexities associated with distribution of daylight in interior spaces is evaluated.

- University of Washington
- College of Built Environments
- Master of Science in Architecture
- Alireza Hashemloo
- Spring 2016

- Thesis Committee Chair: Mehlika Inanici
- Thesis Committee Member: Christopher Meek

Table of Contents

Chapter 1: Introduction

Chapter 2: Annual Daylight Simulation Methodologies

- 2.1 Computer graphics rendering methods in lighting simulation
- 2.2 The Daylight Coefficient Method:
- 2.3 Ray-scattering and BSDF Data
- 2.4 The Three-phase Method
- 2.5 The Five-phase Method

Chapter 3: Research Methodology

- 3.1 Preparation of the simulation scene
- 3.2 The Three-phase simulation process
- 3.3 The Three-phase Direct Solar Component
- 3.4 Simulation of high-precision direct solar contributions
- 3.5 Matrix multiplication process

Chapter 4: Simulation Results

- 4.1 Annual time-series luminance distribution maps
- 4.2 The computational processing times

Chapter 5: Conclusions

- 5.1 Improved accuracy in the prediction of luminance distribution maps
- 5.2 Enhanced comparative evaluation of distinct fenestration systems
- 5.3 Reduced computational processing time
- 5.4 Future Developments

Chapter 1
Introduction

Introduction

Computational simulation methodologies have provided practitioners in the Architecture, Engineering and Construction (AEC) industry, as well as building scientists and researchers in the academic environments, an unprecedented insight to the implications of individual design, engineering and construction strategies on the overall performance of the buildings. The broad landscape of the building performance evaluation incorporates a wide variety of specialization areas such as financial cost and benefits, health and safety, natural resource management and sustainability, etc. A particular set of criteria referenced for a building performance evaluation often engages a number of areas of specialization. For example, the matter of energy consumption loads in a high-rise development is influenced by the occupants' thermal comfort (health and safety), expenditures associated with purchase of energy (financial cost and benefit), the original source of the energy and the efficiency of

mechanical/electrical systems (natural resource management and sustainability), etc.

One of the areas in building performance evaluation under rapid development in the past decade is the daylight simulation. Daylight simulations have been utilized by a number of dedicated experts since 1990s, but recent developments that focus on long term, climate based simulations open up new and exciting research and practice opportunities. While the critical impact of natural daylight on human health and well-being has been substantiated by researches in the area of medical science for a long period of time, it has only been in the past two decades that architects and daylighting specialists in the building design industry have the computational tools and simulation platforms as widely-available to predict the daylight distribution dynamics in their built environments.

A large body of daylight simulation practice for optimization of building facades and development of daylight control strategies, however, have been driven

by performance criteria related to daylight availability, occupant's thermal comfort, solar heat gains and the respective energy consumption loads by HVAC systems. The occupant visual comfort, on the other hand, has not been widely incorporated in the daylight control and building performance optimization strategies.

One reason for such narrow incorporation of visual comfort metrics in development of building performance strategies is that while a large number of form-regulating shading methodologies have been developed based on the presence of direct solar beam at the target daylit space and/or the predicted illuminance-values as the outcome of daylight simulation runs, there has not been a form-regulating shading methodology based on occupant visual comfort. As a result, unlike energy-oriented daylight simulations, the architects and design practitioners do not have the computational workflows or tools that allows for developing a shading solution (as part of the development of a daylight control strategy) that is

exclusively based on occupants visual comfort criteria. The GlareShade (Hashemloo, Inanici and Meek, 2014) is a recent form-generating shading methodology that is exclusively based on occupant visual comfort.

Another major obstacle is that daylight studies were mostly limited to the evaluation of the availability of a certain amount of light on a given task surface. These evaluations are based on predicted illuminance values per sensor point on a target surface area where a set of illuminance values are defined as upper and lower thresholds. For a long period, the predicted illuminance values at a given point in time were evaluated based on a recommended light threshold. The practice of evaluating the predicted illuminance values at a given point in time both with a lower threshold and an upper threshold is a relatively new practice to determine whether the given daylight distribution is as too dim or too bright for the occupant. The assessment of occupant visual comfort is often limited to the specified upper threshold. Such illuminance-based evaluation is too simplistic to address the complexities associated

with human eye perception and individuals' preferences to find a given daylight distribution within a target point of view as discomforting or not. The matter of visual comfort is best evaluated based on luminance values predicted at a target viewpoint for a given point in time.

The existing daylight simulation tools utilized by designers and building sustainability specialists allow for prediction of illuminance values at a set of target sensor points as well as the distribution of luminance values relative to a target point of view at a single point-in-time. However, for a comprehensive assessment of daylight distribution dynamics at a given daylit space, a much broader set of data relative to point-in-time prediction of luminance/illuminance distributions across an entire year is required. These annual predictions of daylight dynamics incorporate the specific climatic features of the geographical project location and the respective impact on daylight distribution patterns during different periods of time across an entire year.

The existing digital simulation platforms allow architects and daylighting practitioners to conduct such climate-based annual prediction of daylight dynamics for illuminance distributions on a set of target sensor point. However, the default operation of these simulation platforms are in general incapable of providing annual luminance distribution data for a target point of view that is required for visual comfort studies. The DIVA-for-Rhino (Jakubiec and Reinhart 2011) is a daylighting simulation platform that provides a visual comfort study on an annual scale for a target viewpoint. The visual comfort analysis metric used in this type of simulation is a simplified version of the Daylight Glare Probability (DGP) (Wienold and Christoffersen 2006; Wienold 2009). While the original DGP provides glare evaluation in single point-in-time simulation from luminance distribution maps, the conducted annual visual comfort analysis (the simplified version) is based on incident illuminance values on a vertical surface at the examined point of view. The applied shift in the referenced data type from

luminance values to illuminance values was due to the absence of an implementation workflow with respect to the existing computational daylight simulation methodologies that are capable of predicting luminance distribution maps across an entire year on a point-in-time basis. This has changed with developments of the Three-phase (Ward et al. 2011; McNeil 2013) and the Five-phase (McNeil 2013) daylighting simulation methodologies that allows us to produce both illuminance and luminance based annual simulations. However, it should be noted that the new and exciting techniques have very steep learning curves, they are still in development phase which makes it challenging to master even for a seasoned daylight simulationist, and requires the deployment of text based commands that are not accessible through graphic user interfaces. Therefore, they are accessible for utilization in a limited manner.

This thesis investigates the existing annual climate-based daylight simulation methodologies for providing time-series luminance distribution data for a specified

viewpoint. Each methodology's capability to simulate the real-world complexities associated with distribution of daylight in interior spaces is evaluated. An implementation workflow for the most advanced annual climate-based daylight simulation methodology (the Five-phase method) based on the existing literature is provided as an explanatory guideline for non-developer designers and daylight practitioners. The individual simulation procedures of the methodology are discussed to provide insight to a powerful, useful, complicated and challenging simulation option. Finally, the primary features of the investigated methodologies and opportunities for future developments are discussed in the conclusions.

Chapter 2
**Annual Daylight Simulation
Methodologies**

2.1 Computer graphics rendering methods in lighting simulation

Two rendering methods commonly used in computer graphics to visualize a digital 3D environment are the Radiosity (Goral, Torrance, Greenberg, Battaile 1984) and Ray-tracing (Appel 1968, Whitted, 1979). Both methods have been utilized in existing lighting simulation platforms and generate quantified results of distribution of daylighting and/or electric lighting in a given environment. The simulation outputs can also be presented as 2D images from user-specified view settings. It is important to note that the capabilities of these rendering algorithms are quite different for simulating the physically based properties of complex materials.

The Radiosity method exclusively accounts for Lambertian reflectance off any surface in the scene that is hit by a ray. Therefore, the definition of material properties for a simulation conducted by the Radiosity method is limited to matte surfaces with a complete

diffuse reflectivity. On the other hand, the assumption of complete diffuse reflection for all surfaces drives the computational processing requirements of the Radiosity method to be independent of the view settings. In other words, any visualization of the scene relative to a particular view setting does not impact the processing time required to calculate the inter-reflections of sample rays between the objects in the scene as the appearance of a matte surface is constant from any point of view.

The Ray-tracing method, by contrast, allows for defining more complex material properties in the scene such as glossy and/or translucent materials that are driven by specular reflectivity. The Ray-tracing method presents a robust capability to account for any hybrid reflectivity (i.e. directional and diffuse) behavior defined for a given object. The appearance of an object with specular or directional diffuse reflectivity is dependent on the point of view. In other words, the visualization of a specular surface at a point in time by two separate viewpoints could be dramatically different. The ability

to simulate both specular and directional diffuse materials in the scene impacts the computational processing requirements (such as the total rendering time) for a Ray-tracing based simulation. Multiple viewpoints would equate to multiple renderings.

The accuracy lighting simulation results (such as the illuminance values on a target sensor point or the distribution of luminance values within a target viewpoint) is critical for informed design decision making and comparative performance analysis with respect to a set of criteria (such as the occupants' visual comfort and/or energy consumption efficiency).

While benefiting the accelerated rendering process, the limitations of the Radiosity method to account for non-matte material properties leads the accuracy of simulation results using the Radiosity method to be insufficient for informed design decision making or performance evaluations of common architectural settings. For instance, Radiosity method will not be

adequate to evaluate the students' visual comfort in a classroom with translucent skylights.

Accounting for specular and directional diffuse reflectivity, the Ray-tracing method is utilized in lighting simulation engines such as the Radiance Lighting Simulation and Visualization software (Ward 1994; Ward and Shakespeare 1997) with validated simulation results against real-world measurements (Mardaljevic, 1995). Regardless of other contributing factors for the overall reliability of the consequent simulation data (such as the user-defined simulation assumptions) the simulation results based on the Ray-tracing method are principally accepted as sufficiently accurate for reliable performance analysis and design decision making. Although the unsolicited increase in processing time for a limited number of singular point-in-time simulations using the Ray-tracing method can be identified as acceptable (considering an average hardware specification for a workstation computer), it turns into a major impediment for a substantial number of point-in-time simulations.

Computational processing time: a major impediment in time series lighting simulation

Using Radiance as a validated lighting simulation software based on backward ray-tracing, the level of accuracy of simulation results is dependent on the user-defined description of the simulation environment and the specified rendering settings. The reliability of consequent data by the lighting simulation is commonly determined by pre-defined “acceptable” level of accuracy according to the scope of corresponding design phase and/or the sensitivity of metrics targeted in a comparative performance analysis. Various researchers report error margins within 20% as expected and acceptable (Mardaljevic, 2000; Ibarra and Reinhart, 2009).

With a non-complicated simulation scene (no complex shading geometry or hybrid/directional diffuse specular reflectivity as part of assigned material properties) and lower rendering settings such as using a value of 3 for ambient bounces, one can simulate the illuminance

values for a desired number of sensor points at a single point in time or generate a simulated High Dynamic Range (HDR) image that represents luminance value per pixel relative to a single viewpoint with sufficient accuracy for preliminary design studies. By enhancing the rendering settings such as increasing the value of ambient bounces to 6, the required computational processing time will also be increased. The “accuracy” of this set of data, however, may not have been significantly different, in comparison with the previous set, given the absence of complex geometry or material properties in the scene. However, the user should be cautious: this basic assumption is easily violated, for example, in the presence of blinds, where the light distribution in the scene is dependent on multiple reflections.

Trading the negligibly improved accuracy with significantly accelerated processing, such simulation can be conducted for a limited number of points in time. However, the required processing time even for even simplified simulation scenes and rendering settings

becomes a liability for greater number of point-in-time simulations such as hourly illuminance data throughout the entire year. The problematic simulation time will be dramatically increased once higher rendering settings must be assigned to meet the desired level of accuracy in response to the application of more complex geometries and material properties in the scene.

The impediment of increased computational processing time for substantial number of point in time simulations has led to the introduction of lighting simulation methods based on the concept of Daylight Coefficients.

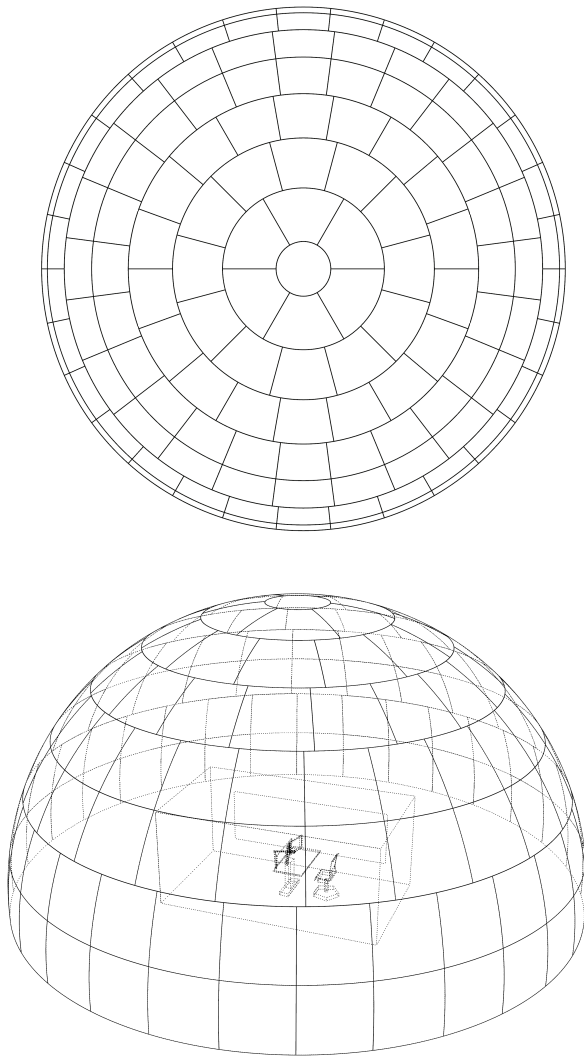


Figure 1: Tregenza Sky Subdivision Model

2.2 The Daylight Coefficient Method:

The Daylight Coefficient is defined as the calculation of daylight contribution from individual segments of a subdivided sky dome relative to a target sensor point or point of view. The concept of Daylight Coefficient was first introduced by Tregenza and Waters (1983). According to Tregenza's daylight coefficient model, the sky dome is subdivided into 145 sky patches.

(Figure 1)

The daylight coefficient of sky patch (n) relative to a single sensor point (X) on a task plane is equal to the measured illuminance value at the sensor point divided by the product of the luminance of the sky patch and its respective angular size (Figure 2, Equation 1). In other words, DC determines the contribution of each individual sky patch on the illuminance of a sensor point. The total illuminance of a single sensor point, therefore, will be equal to the sum of the products of daylight coefficient, irradiance and angular size per individual sky patch (Equation 2)

$$DC_{(n)}(X) = \frac{E_{(n)}(X)}{L_{(n)}S_{(n)}}$$

$DC_{(n)}(X)$: Daylight Coefficient at sensor point (X) relative to the sky patch (n)

$E_{(n)}(X)$: Illuminance value at sensor point (X) relative by sky patch (n)

$L_{(n)}$: Irradiance of the sky patch (n)

$S_{(n)}$: Angular size of the sky patch (n) from sensor point (X)

Equation 1

$$E_{(X)} = \sum_{n=1}^{145} DC_{(n)}(X) L_{(n)} S_{(n)}$$

$E_{(X)}$: Total illuminance value at sensor point (X) by the entire sky dome (145 sky patches)

Equation 2

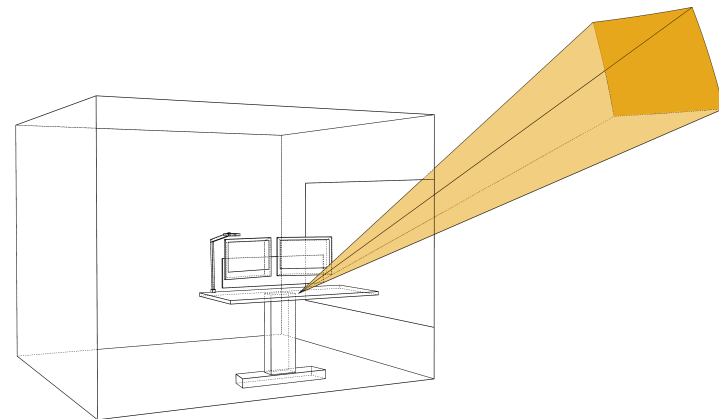
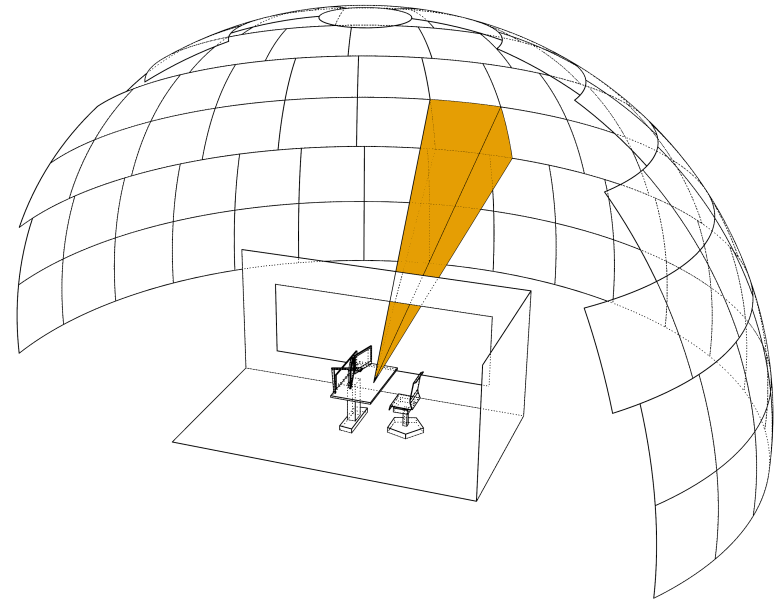


Figure 2

Using Radiance for point-in-time simulation of illuminance values at a number of sensor points, the sky model along with all other material properties and object geometries in the scene are processed as part of the Ray-tracing algorithm to predict the targeted illuminance values. Once this simulation is conducted for a different point in time, the entire Ray-tracing process is independent from the previous simulation and it is fully repeated. As described in the previous section, once the number of point in time simulations increases, the required rendering time will become an obstacle. The number of daylight hours in a location varies between 3500-4000 hours depending on location. The fundamental idea behind the Daylight Coefficient method is to bypass this repetitive implementation of Ray-tracing method for any number of simulations and use a package of 145 simulations to compute Daylight coefficients, which can be subsequently used to determine any number of simulations as quick post processes. Therefore, the technique allows us to generate long term data with significantly shorter processing times.

Following its first introduction by Tregenza and Waters (1983), several Daylight Coefficient models have been proposed with validated results for sequential point-in-time simulations (Tsangrassoulis and Santamouris 1997, Mardaljevic 2000, Reinhart 2001, Reinhart and Walkenhorst 2001, Reinhart and Andersen 2006). The presented approach of these models to account for diffuse sky contributions are fundamentally similar. The primary difference in these methods are their approaches towards calculating solar contributions.

The Standard Daylight Coefficient Model for Dynamic Daylight Simulations (Bourgeois, Reinhart and Ward 2008) proposes an integrated approach based on the previously proposed methods. The significance of the standard daylight coefficient model is that it introduces a concept of computational data format that has been functionalized, to a great extent, in Radiance. The proposed standard daylight coefficient model for simulating diffuse daylight contributions along with the solar contribution is as follows:

$$E_{Diffuse\ Sky} = \sum_{n=1}^{145} DC_n L_n S_n$$

$$E_{Diffuse\ Ground} = DC \times L \times S$$

$$E_{Total\ Diffuse} = E_{Diffuse\ Sky} + E_{Diffuse\ Ground}$$

E_{Sky} : Diffuse sky contribution

E_{Ground} : Diffuse ground contribution

E_{Total} : Total sky and ground diffuse contributions

Equation 3

Diffuse sky and ground contributions:

Tregenza's original sky subdivision model (Tregenza 1987) has 145 sky patches with circular outline that partially covers the entire sky dome. While following an identical number of sky patches, the applied sky subdivision algorithm in the standard model (Bourgeois et al. 2008) is based on the subdivision scheme used in Daysim (Reinhart 2001) with rectangular outline for individual sky patches that results in complete coverage of the sky dome.

A single patch is added for the ground to simulate the diffused daylight reflected off its surface. As a result, the total diffuse sky and ground contributions are equal to the sum of the products of daylight coefficient, irradiance and respective angular size per individual sky patch and the ground. (Equation 3)

Solar Contributions:

The solar contributions in the standard model (Bourgeois et al. 2008) are categorized as direct and indirect contributions. The direct solar contributions refers to the incidence of direct rays from the sun on the target sensor point. The indirect solar contributions, on the other hand, is referred to all solar rays reflected off surrounding surfaces in the scene before hitting the target sensor point.

To identify the accountable patches for indirect solar contributions, the subdivision method resulting in 145 sky patches is used in a similar fashion to calculate the diffuse sky contributions. According to the position of the sun in the sky driven by the simulated point in time, the center point of four adjacent patches circumventing the exact location of the sun are identified. The indirect solar contribution is distributed to these four sky patch center points. The distribution process is interpolated according to a weight factor assigned to each point that is driven by its proximity to the exact location of the sun

$$E_{\text{Indirect Solar}} = \sum_{n=1}^{145} W_n DC_n L_n S_n$$

W_n : interpolated weight assigned to individual sky patches.

Equation 4

$$(144 \times 16) + 1 = 2305$$

Equation 5

in the sky dome. The sky patch with a center point in closer proximity with the sun position gains a higher weight for the distributed solar contributions. As a result, the total indirect solar contributions for a given sensor point are equal to the sum of the products of the interpolation weight, irradiance and the respective angular size of the four patches. The indirect solar contributions for remaining 141 patches is considered as 0. (Equation 4)

The computation process for the direct solar contributions is similar to the one used for the indirect contributions. The main difference is that a higher number of sky dome subdivisions is referenced. A subdivision value of 2305 is utilized in the standard model that is driven by quadrupling all sky patches in the original 145 division scheme with an exception of the single patch corresponding with the zenith. (Equation 5)

The increased number of subdivisions results in a higher accuracy that is necessary to determine

whether a sample ray from one of the four interpolated center points of the sky patches will directly hit the target sensor point at a given point in time. The total direct solar contributions are equal to the sum of the products of interpolation weights, irradiance and respective angular size of the four patches where contribution by the remaining 2301 patches is considered as 0. (Equation 6)

$$E_{Direct\ Solar} = \sum_{n=1}^{2305} W_n D C_n L_n S_n$$

Equation 6

$$E_{Total} = E_{Total\ Diffuse} + E_{Indirect\ Solar} + E_{Direct\ Solar}$$

Equation 7

Total Daylight Contributions:

Based on the described calculation procedures, the total daylight contributions in the standard daylight coefficient model is equal to the sum of the total diffuse sky and ground contributions and the total direct and indirect solar contributions. (Equation 7)

2.3 Ray-scattering and BSDF Data:

The transmissivity of a specular object (such as the glass pane in a window assembly unit) can be specified as part of a Radiance material definition. The assigned material properties relative to the object's transmissivity, however, is valid for rays hitting the object's surface on a perpendicular angle.

Therefore, simulations using the basic Radiance material definition for the glazing surfaces (i.e. glass material type) do not account for the "ray-scattering" behavior of the specular objects that is identified as the reflection and transmission with dissimilar energy flux and direction (three-dimensional geometric properties) in comparison with the original incident ray. While the outcome of such simulations could present the general dynamics of distributed daylight in the simulation scene, the simulation results are identified as too simplistic to account for the impact of the optical properties pertaining to the specific specular

fenestration layers through which the energy flux is passed from the exterior to the interior space.

The problem is significant when Complex Fenestration Systems (CFS) identified as window assemblies with specular shading devices (venetian blinds, roller fabric shades, etc.) are used as part of the incorporated daylight control assembly in the space: although it is possible to develop 3D models in the simulation scene representing the shading devices' three-dimensional geometry (such as the slats of a venetian blind assembly), the regular backward ray-tracing simulation process in Radiance may not effectively calculate the inter-reflections and transmissions that occur between the layers of the fenestration system before a ray is passed to the interior space. The backward ray-tracing simulation in the Daylight Coefficient method executed to calculate the daylight contribution coefficients also share this deficiency, and therefore, the outcome of the time-series simulation do not reflect the ray-scattering behavior that is specific to the fenestration system(s) in the scene.

Addressing such deficiency in the backward ray-tracing simulation runs via Radiance, the Bi-directional Scattering Distribution Function (BSDF) data descriptive of the ray-scattering behavior of a given specular object is incorporated as part of a simulation process titled as the “Three-phase” method (Ward et al. 2011; McNeil 2013) . The concept of ray-scattering is developed to increase the accuracy of simulations of incident light rays on specular objects along with the structure of BSDF data in the Three-phase method.

Ray-scattering: transmission and reflection of incident luminous flux by specular objects

The luminous flux diffused by the atmosphere or sustaining its radiation path from the sun follows a linear motion track from the origin of departure until it hits the surface of a physical body. Prospective immediate outcomes of an incident ray with a specular object, such as the glazing surface of a window assembly, include reflection, absorption and transmission. The likelihood of each outcome and the extent to which one outweighs the others (in terms of the amount of energy it assimilates relative to the total amount of energy carried by the flux just before the incident) varies greatly depending on the optical properties of the object. A regular glass pane as part of window assembly unit will produce all three outcomes when hit by a light ray.

Considering a single point of incidence on a given glazing surface (Figure 3), the angle (α), defined as the angle between the path of incoming ray and the

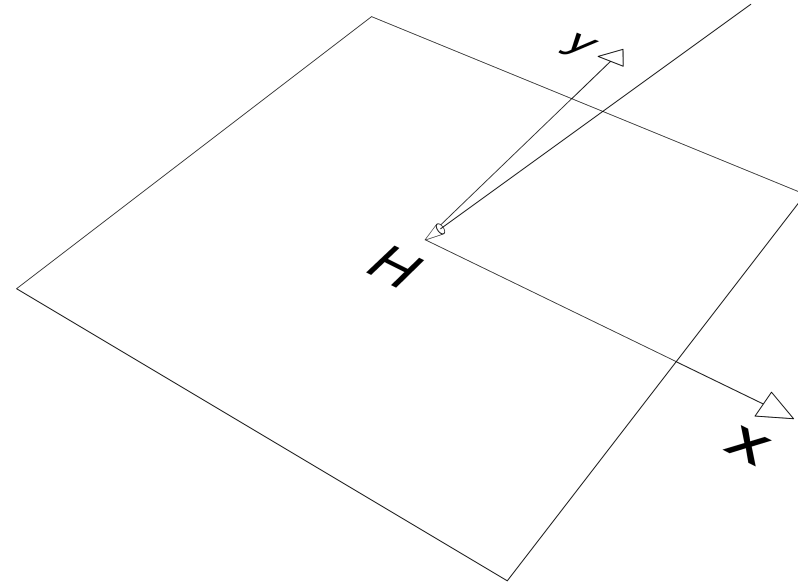


Figure 3: Incident ray and the 2D coordinate system at the point of incidence

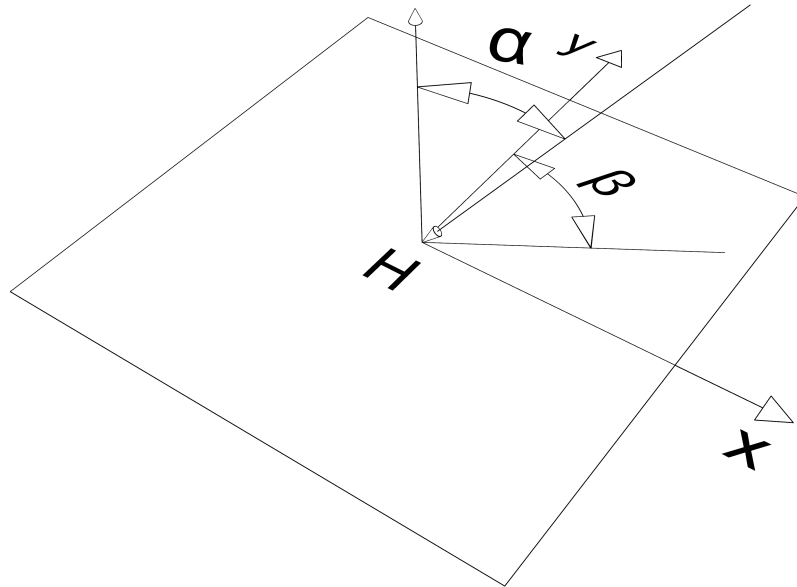


Figure 4: The three-dimensional directional properties of an incident ray is described by the (α) and (β) angles.

surface's normal vector, varies within a range of values greater than or equal to 0° and less than 90° . In order to specify the exact geometric properties of the incident ray in the three-dimensional space, a second geometric property must be also defined. Given a Cartesian coordinate system with X and Y axis that is coplanar with the physical object's surface, the angle (β) is defined as the angle between the projection of the incident ray on the surface (along the surface's normal vector) and the Y axis; angle (β) varies within a range of 0° and 360° . Referencing both (α) and (β) angles, it is possible to define the exact geometric properties of a given incident ray on the surface of the object in three-dimensional space. (Figure 4)

The value of $\cos(\alpha)$ (relative to the surface's normal vector) determines the amount of incident energy that passed through to the transparent object. As the range of possible values for (α) is between 0° and 90° , the object will obtain the maximum amount of energy flux that it can physically receive at a given environment, if (α) is equal to 0° (the ray is perpendicular to the

surface). On the other hand, the total amount of energy flux passed to the object will be minimized at an identical physical environment if (α) is marginally less than 90° (the ray is almost parallel to the surface).

If (α') is supplementary with (α) , relative to $(r1)$ and $(r2)$ as two incident rays with identical energy flux, respectively, the amount of energy passed to the object by the two rays will be equal considering the absolute value of $\cos(\alpha')$ is equivalent to $\cos(\alpha)$.

The value of (α_t) and (β_t) as the geometric properties defining the direction of the transmitted ray leaving the specular object on the opposite side of the incidence surface, however, is not necessarily identical with (α) and (β) corresponding with the geometric properties of the incident ray's direction. Such variation is also applicable to the geometric properties of the ray reflected off the incidence surface back to the outside environment with those of the incoming ray. In order to account for the ray-scattering behavior of a fenestration assembly in a computational daylight and

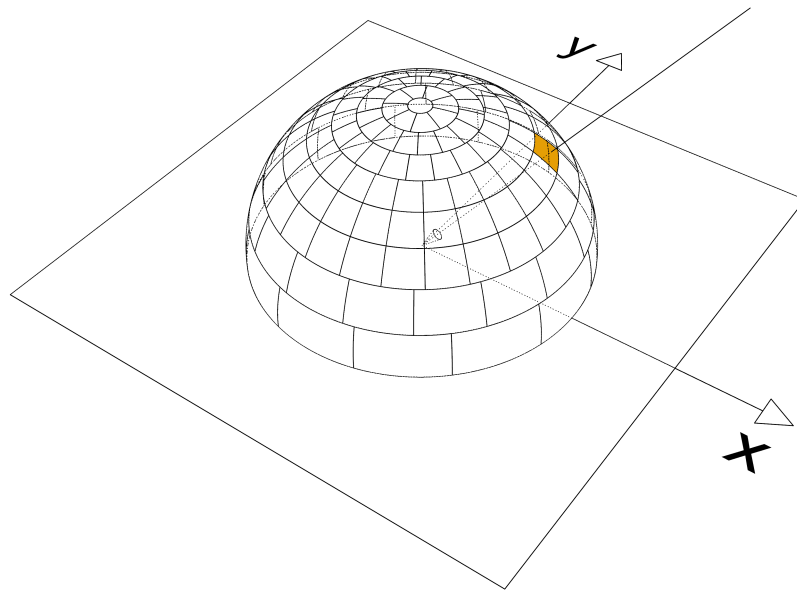


Figure 5: The Klems' coordinate system is comprised of a hemisphere in three-dimensional space that is subdivided into 145 patches. A single Klems' patch describes a range of possible values for (α) and (β) angles.

energy simulation, a new coordinate system must be deployed to properly address all possible variations between the incident ray's geometric properties and those of the reflected/transmitted rays. The Klems' coordinate system (Klems 1994a and 1994b) was first developed to address this demand as a way of specifying the ray scattering behavior of window glazing surfaces relative to the solar heat gains.

The Klems' coordinate system is comprised of a hemisphere in three-dimensional space where a hypothetical vector defined between the zenith and the center of the hemisphere is perpendicular to the object's surface at the point of incidence. (Figure 5)

Considering (α) and (α') relative to incident rays ($r1$) and ($r2$) with equal energy flux where ($\alpha = \alpha'$), the total amount of energy flux passed to the surface of incidence by the two rays is equal as well. Such identical transfer of energy flux by two incident rays is independent of the rays' respective (β) angle value. In other words, any number of incident rays with identical

energy flux and (α) angles will transfer an identical amount of energy per ray while the corresponding (β) angle value varies within a range of 0° and less than 90° . The independence of the energy flux transfer from the ray's (β) angle value identifies the ray's (α) angle value as the only component among the ray's three-dimensional geometric properties that impacts the total amount of energy flux transfer to the surface of incidence.

Given the range of possible values for (α) and (β) as $[0,90)$ and $[0,360)$, respectively, accounting for all possible three-dimensional properties of an incident ray results in 32,400 (90×360) possible permutations of (α) and (β) with an interval of 1° between each two consecutive values for (α) and (β).

The range of possible values for (α) is subdivided into 8 intervals in the Klem's coordinate system where the middle value of each interval is referenced to represent the entire interval. As a result, the incident rays with different (α) angle values within the same interval are

referenced with a single (α) value that is equal to the middle value of the corresponding interval.

The Klems' coordinate system implements such classification of (α) values into 8 discreet intervals through the subdivision of the hemisphere via "θ bands" as eight concentric circles projected on the hemisphere along the incidence surface's normal vector. Such subdivision allows for accounting for all possible values for (α) (and (α') as its supplementary angle in the three-dimensional space) via only 8 possible values.

While the exclusive application of this subdivision is sufficient to address the variations in the amount of energy delivered by a ray relative to the corresponding (α) value, the (β) property of the incident ray is not addressed. The specification of both (α) and (β) angles as part of the computational ray sampling process is critical: the geometric properties of the incident ray is used to determine the geometric properties of the reflected and transmitted rays based on the object's

ray scattering behavior. For example, the geometric properties of the transmitted ray is particularly necessary to determine the next point of the ray's incidence on an interior surface in the simulation scene.

Responding to the sampling demand for all possible (β) values in the three-dimensional space, individual θ bands in Klems' coordinate system are further subdivided via projected horizontal lines intersecting at the center of the hemisphere. As a result, each θ band is subdivided into four-sided regions each called a "patch". The number of consequent subdivision patches vary across the θ bands so that all 145 consequent patches (including the zenith as a single patch) have equivalent $\cos(\alpha)$ -weighted solid angles.

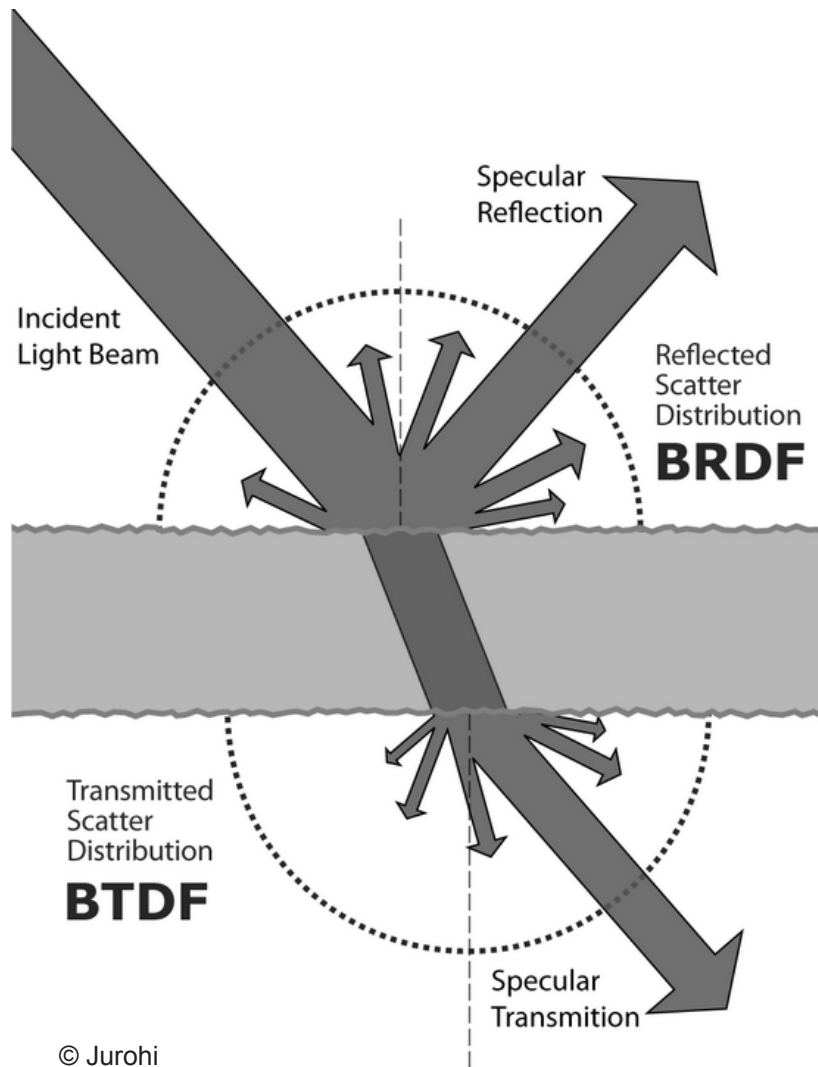


Figure 6: The BSDF data describes the ray-scattering behavior of a specular object driven by its optical properties.

Bi-directional Scattering Distribution Function (BSDF) Data:

The ray-scattering behavior of a specular object driven by its optical properties determines the geometric properties of both the reflected and transmitted rays relative to an incident ray. A single BSDF data set representing this ray-scattering behavior, therefore, can be separated into two discrete data sets: Bi-directional Transmittance Distribution Function (BTDF) and Bi-directional Reflectance Distribution Function (BRDF). (Figure 6)

Similar to the incident ray path, the geometric properties of the reflected and transmitted rays can be defined via a single patch using the Klems' coordinate system setup as two concentric hemispheres at the point of incidence: i) one hemisphere at the exterior side of the glazing surface to define the geometric properties of the incident ray as well as the reflected ray and ii) another hemisphere at the interior side to

define the geometric properties of the transmitted ray. (Figures 7-8)

Using Radiance for simulation of daylight dynamics at a given interior space, the reflected rays off the glazing surface(s) back to the outside environment do not impact the distribution of daylight at the interior spaces. As a result, the Radiance only uses the BTDF data to account for the ray scattering behavior of the fenestrations systems relative to the transmitted rays into the daylit space.

For a given transmitted ray, there are 145 Klems patches to account for all possible geometric properties of the corresponding incident ray in the three-dimensional space. In other words, considering a single transmitted ray with the hypothetical geometric properties corresponding with patch (p) in the Klems' hemisphere on the interior side of the fenestration system, there will be 145 possible permutations between patch (p) and a single patch from the Klems' hemisphere on the exterior side of the fenestration

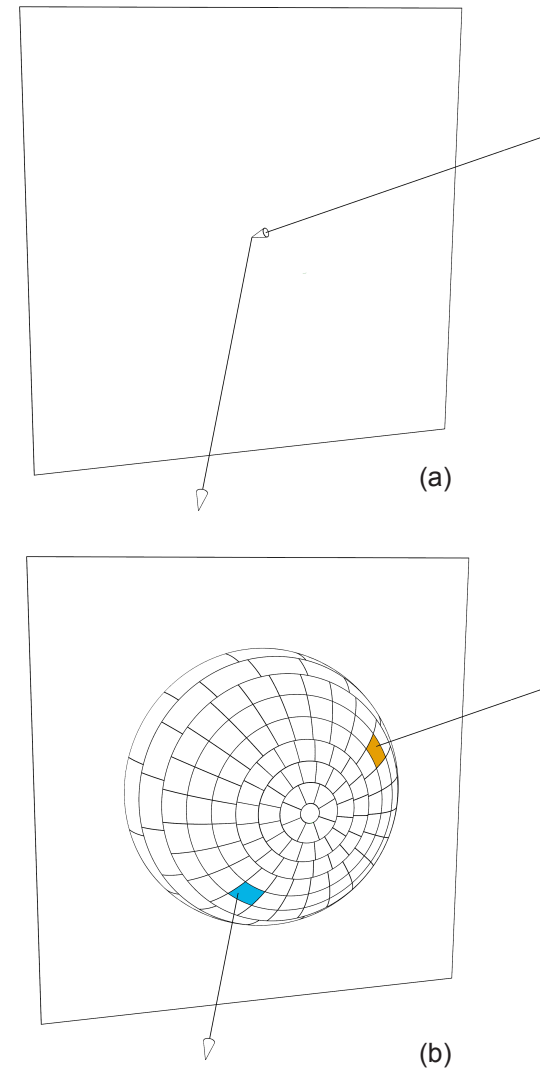


Figure 7: (a) Incident ray and the corresponding reflected ray
(b) Klems' patches describing the direction of the incident ray and the reflected rays

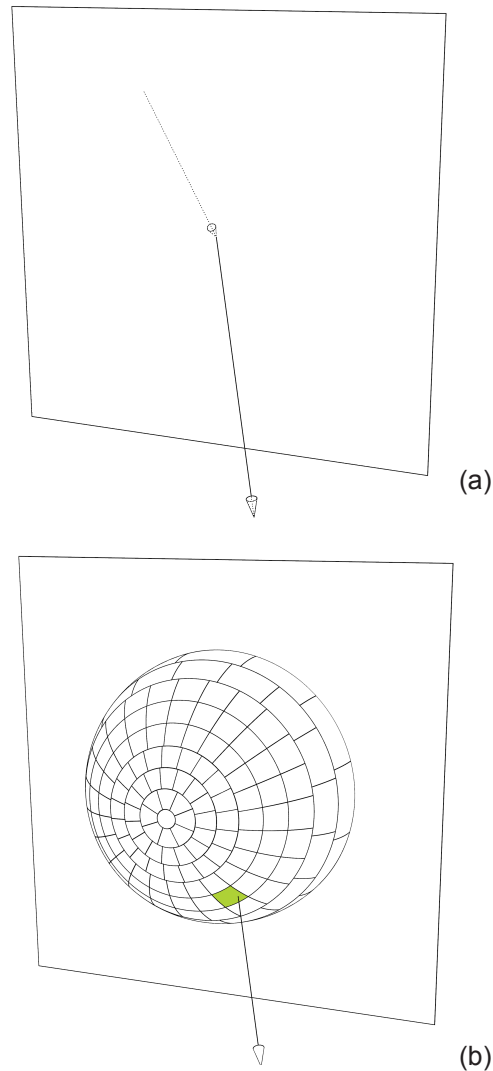


Figure 8: (a) Incident ray and the corresponding transmitted ray
 (b) Klems' patch describing the direction of the transmitted ray

system that is used to define the incident ray's geometric properties. The amount of energy the transmitted ray would assimilate relative to the total amount of energy that was carried by the incident ray is not constant between all 145 permutations. Consequently, a transmittance coefficient can be defined for each 145 permutation as a result of dividing the assimilated amount of energy of the transmitted ray by the total amount of energy that was carried by the incident ray just before hitting the object's surface.

As a result, using the Klems' coordinate system, there will be a total number of 21,025 (145×145) possible permutations of the geometric properties relative to a pair of transmitted ray and its corresponding incident ray. A single BTDF data set consists of a 145 by 145 matrix of transmittance coefficients to account for all these 21,025 possible permutations. Individual transmitted and incident ray patches correspond with a single column index and a row index, respectively, of the BTDF matrix. As a result, the total energy of light ray that corresponds with the transmittance patch (p)

will be equal to the sum of the products of the energy carried by the incident light ray along each individual incidence patch and the corresponding transmittance coefficient (Saxena et al. 2010) (Equation 8)

$$E_m = \sum_{n=1}^{145} C_{mn} E_n$$

E_m: the amount of energy carried by the transmitted light ray at the row index (*m*) of the BTDF matrix

E_n: the amount of energy carried by the incident light ray at column index (*n*) of the BTDF matrix

C_{mn}: the transmittance coefficient corresponding to the transmitted light ray at row index (*m*) relative to the incident light ray at column index (*n*) of the BTDF matrix

Equation 8

2.4 The Three-phase Method:

Using the Daylight Coefficient method, it is possible to simulate the illuminance of a set of target sensor points and/or the luminance distribution relative to a target point of view in constant time intervals across an entire year. However, the daylight coefficient method refers to the regular Radiance material definition for a “glass” modifier that is assigned to the polygon(s) in the simulation model representing the glazing surfaces. The assigned Radiance material definition for “glass” simplifies the ray scattering behavior of the glazing surfaces that is driven by the specific optical properties of the glass product used in the fenestration system. In addition, the individual back-ward raytracing simulation runs that are executed to calculate the daylight contribution by individual sky patches, do not have the capability to properly account for the ray scattering behavior of any non-specular shading devices installed as part of the fenestration systems in the daylit space.

The Three-phase method (Ward et al. 2011) as a validated simulation methodology (McNeil and Lee 2012) incorporates the BTDF data with the Daylight Coefficient method to account for the ray scattering behavior of the fenestration system(s) as part of the simulation of daylight dynamics at a given daylit space across an entire year.

Using the Daylight Coefficient method, the predicted illuminance value at a target sensor point relative to the daylight contribution of an individual sky patch is equal to the product of the corresponding daylight coefficient and the irradiance of the sky patch at the given point in time. The Three-phase method identifies three coefficients that replace the (C) value in the Daylight Coefficient method's equation: the view coefficient (matrix), the transmittance coefficient (matrix) and the daylight coefficient (matrix). (Figure 9)

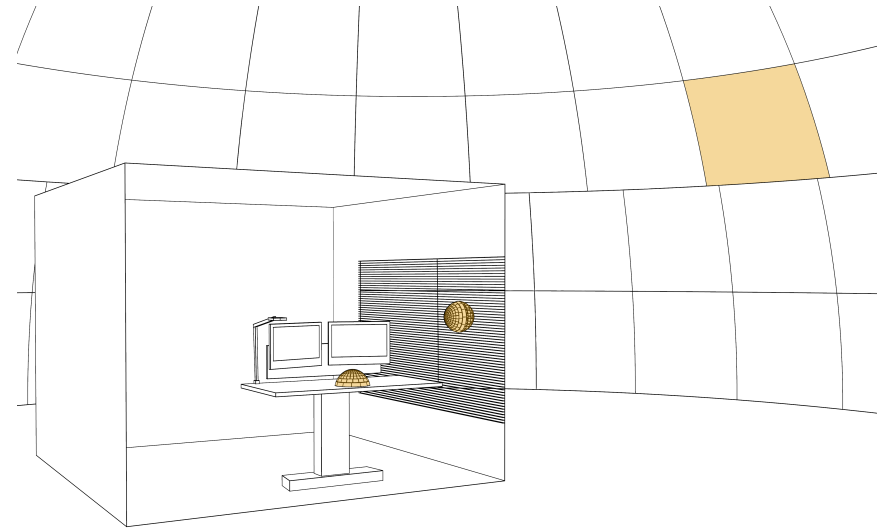


Figure 9: in the Three-phase method, the luminous flux transfer for a given sky description from outside to target sensor point at the interiors is defined by three matrices: Daylight Matrix, Transmission Matrix and the View Matrix

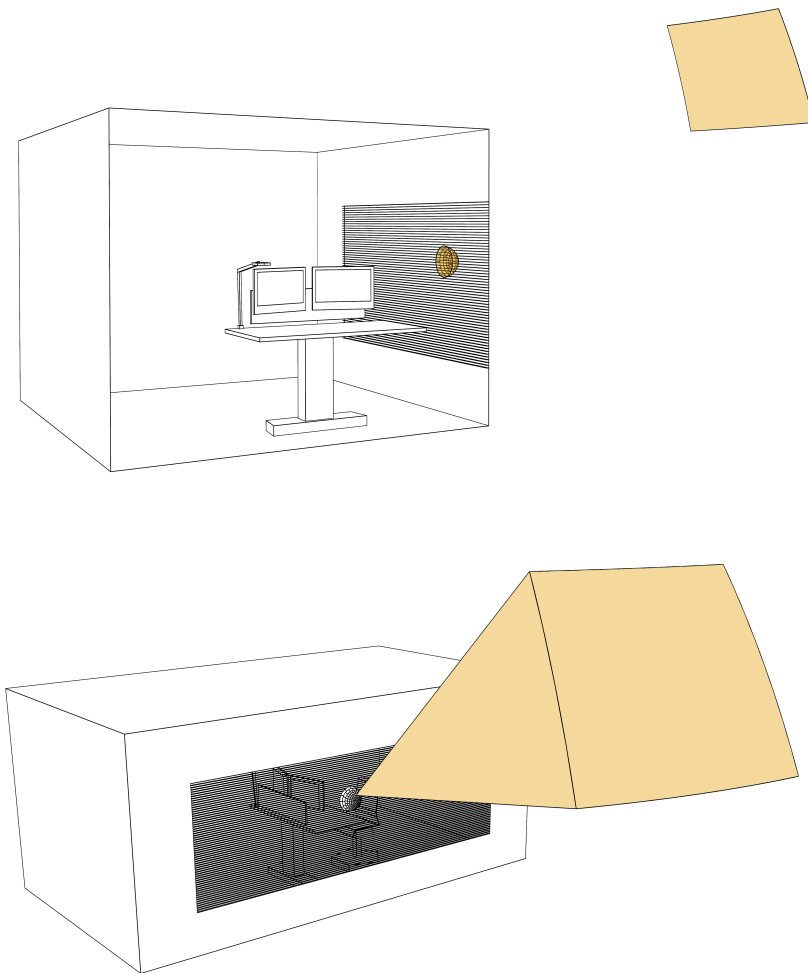


Figure 10: Daylight Matrix: relating sky patches to incident rays on the glazing surface based on Klems' coordinate system

The Daylight Coefficient Component:

While sharing an identical title, the actual definition for the daylight contribution coefficient (matrix) in the Three-phase method differs from its counterpart in the original Daylight Coefficient method: in the original Daylight Coefficient method, a single coefficient directly relates the contribution of daylight by an individual sky patch to the measured illuminance at the target sensor point in the interior space. A single daylight coefficient in the Three-phase method, on the other hand, relates the daylight contribution by a single sky patch to the luminous flux received by an individual Klems' patch for the incident rays from the outside environment on the glazing surface. (Figure 10)

Using Tregenza's subdivision scheme for the sky dome, the total number of contribution coefficients calculated in the Daylight Coefficient method for a single sensor point will be equal to 145 (1×145). By contrast, the total number of daylight contribution coefficients calculated in the Three-phase method for

a single sensor point using Tregenza's subdivision scheme will be equal to 21,025 ($1 \times 145 \times 145$). In other words, there are 21,025 possible permutations coupling a single Klems' patch for incident rays and a single Tregenza's patch of the sky dome subdivision. Accounting for all these possible permutations as part of the ray sampling process in Radiance, the calculated daylight coefficients in the Three-phase method can be organized in a 145 by 145 matrix where each row and column represents an individual Klems and Tregenza patch, respectively. This matrix of daylight contribution coefficients relating the sky patches with the incident ray patches on the glazing surface is called the "Daylight Matrix" in the Three-phase method.

The Transmittance Coefficient Component (Matrix):

As described in the previous section, a single transmittance coefficient is available from the BTDF data set per individual pair of incoming and outgoing

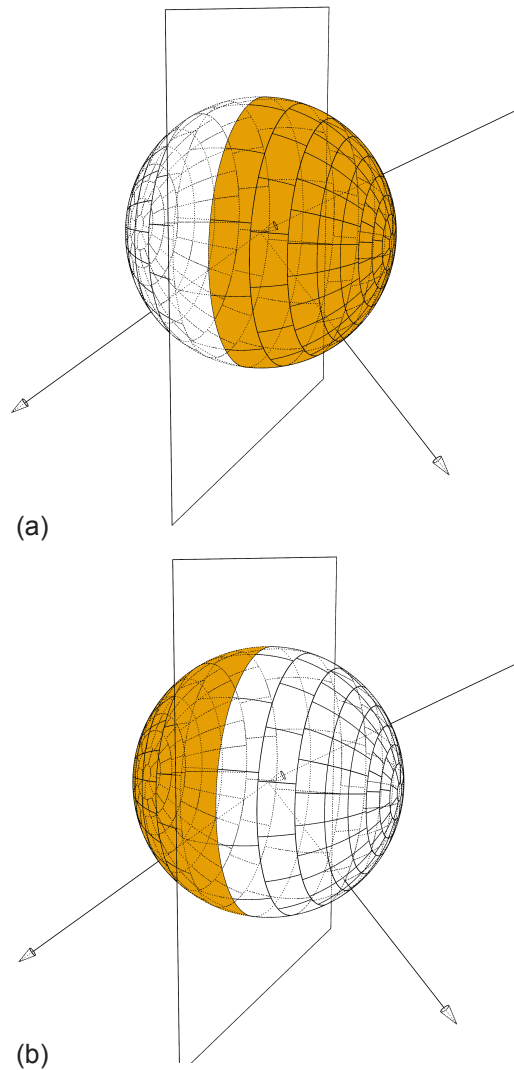


Figure 7: (a) 145 Klemes' patches on the front side describe the directional properties of the incident ray (and the reflected ray)
 (b) 145 Klemes' patches on the back side describe the directional properties of the transmitted ray

patch relative to the Klemes' coordinate system. The 145 by 145 matrix that includes these transmittance coefficients driven by the specific ray scattering behavior of the fenestration system is called the "Transmittance Matrix" in the Three-phase method. (Figure 11)

The View Coefficient Component (Matrix):

Utilizing the Klemes' coordinate system, it is also possible to account for any prospective geometric property of a single transmitted ray that is incident on a target sensor point. Such implementation of the Klemes' coordinate system on the sensor point results in 145 patches through which the surrounding three-dimensional space can be viewed. The contribution of each view patch to the measured illuminance at the target sensor point, however, is not constant across the entire hemisphere of the view subdivision. For example, the measured illuminance value by the transmitted ray (r_1) that is incident on the sensor point through the zenith patch of the view subdivision is

greater than the measured illuminance value by the ray (r_2) with identical luminous flux that is incident on patch 145 ($\cos(\alpha_{r1}) > \cos(\alpha_{r2})$). As a result, a single “view coefficient” can be defined per individual patch. (Equation 09)

The total number of possible permutations pairing a single patch from Klems’ coordinate system for transmitted rays from the fenestration system and a single view patch relative to the sensor point (or point of view) is equal to 21,025 (145×145). The matrix that includes all these view coefficients is called the “View Matrix” in the Three-phase method. (Figure 12)

Prediction of illuminance/luminance distribution using the Three-phase method:

The original Daylight Coefficient method is essentially a two-phase process: i) calculating the daylight contribution coefficients per individual sky patch relative to the examined sensor point and ii) multiplying

$$I_{(n)} = C_{v(n)}E_r$$

$I_{(n)}$: predicted illuminance value contributed by the view patch (n)

$C_{v(n)}$: the view coefficient corresponding with the view patch (n)

E_r : the luminous flux of the transmitted ray (r) that is incident on the sensor point

Equation 9

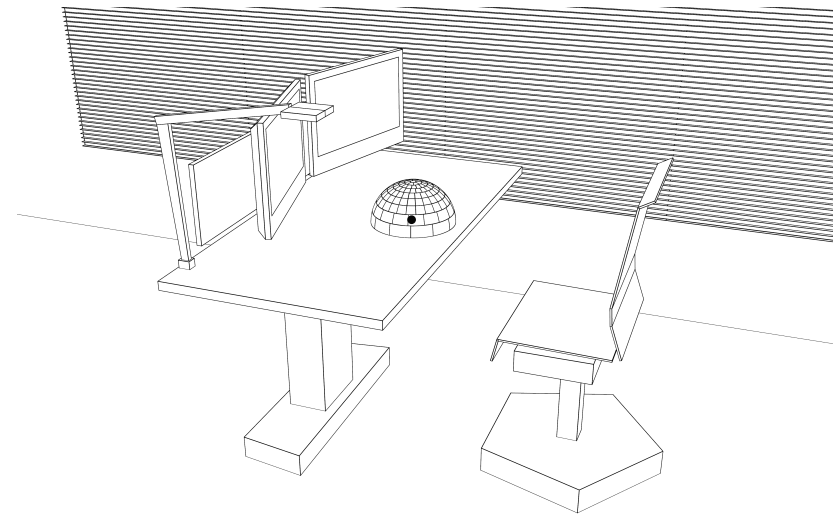


Figure 12: Klems’ directional subdivision model at the target sensor point

each daylight coefficient with the irradiance of the corresponding sky patch at the given point in time to reach the total illuminance value at the sensor point via summing the outcomes of all the multiplications (Tregenza and Waters, 1983; Bourgeois et al., 2008).

With the added capability of accounting for the ray scattering behavior of the fenestration system(s) in the simulation scene, the Three-phase method is a three step simulation process to predict the total illuminance on a target sensor point or the luminous distribution at a target point of view: i) reporting for all possible ray sampling permutations between the sky patches and the fenestration system's coordinate system for incoming rays (Daylight Matrix), ii) addressing the fenestration system's ray scattering function (Transmittance Matrix) and iii) accounting for any prospective ray leaving the fenestration system and falling on the target sensor point or reflecting off the surfaces within the examined point of view (View Matrix) (Ward et al., 2011).

The predicted illuminance of a single sensor point by the Three-phase method at a given point in time will be equal to the product of the view, transmittance and daylight matrices that is multiplied by the irradiance of the sky dome. (Equation 10)

Matrix multiplication operation in the Three-phase method:

The Daylight Coefficient method has been utilized as a computationally-efficient way to simulate the daylight dynamics at interior daylit spaces across an entire year. As described in the previous section, the primary advantage of the Three-phase method to the original Daylight Coefficient method is the capability to account for the specific ray scattering properties of the fenestration system(s) as part of the simulated daylit scene. Using the Three-phase method, the primary time consuming computational processes relate to the calculation of View, Transmittance and Daylight matrices. The distributed luminous flux across the entire sky dome can be modeled per point in time via

$$E_i = VTDE_S$$

E_i : predicted illuminance value on the target sensor point at the given point in time

V : View Matrix

T : Transmittance Matrix

D : Daylight Matrix

E_S : The irradiance of the sky dome at the given point in time

Equation 10

$$A_{(m \times k)} B_{(k \times n)} = C_{(m \times n)}$$

A_(m×k): matrix A with (m) rows and (k) columns

B_(k×n): matrix B with (k) rows and (n) columns

C_(m×n): the product of matrices A and B with (m) rows and (n) columns

Equation 11

the direct normal and diffuse horizontal irradiance values that are available as part of the hourly weather data. Once the coefficients in the three matrices are calculated, the simulation result will be an outcome of a matrix multiplication operation based on the modeled sky description per point in time. The pre-condition to calculate the product of two matrices is that the number of columns in the first matrix is equal to the number of rows in the second matrix. If matrix C is considered as the product of matrices A and B, the dimension of the matrix C will be equal to the number of rows in the matrix A by the number of columns in matrix B. (Equation 11)

Utilizing the Klems' coordinate system for both the incoming and outgoing rays relative to the fenestration assembly, the corresponding BTDF data results in a Transmittance Matrix with equal number of rows and columns (145 × 145). Therefore, as long as the number of columns in View Matrix and the number of rows in the Daylight Matrix are equal to the number of rows and columns in the Transmittance Matrix, respectively, it is

possible to replace the BTDF data set relative to a particular fenestration assembly with another one without the need to re-calculate the View and Daylight matrices. As a result, with a constant Transmittance Matrix dimension, any number of BTDF data sets can be inserted to the Three-phase method's equation (one BTDF data set at a time) to study the impact of the corresponding fenestration assembly on the distribution of daylight in the scene.

It is important to note that the number of columns in the Daylight Matrix corresponding with the applied subdivision scheme to the sky dome is also customizable in the Three-phase method. For example, using the Reinhart's sky subdivision scheme (Reinhart 2001) quadrupling each Tregenza's patch, the dimension of the View and Transmittance matrices in the Three-phase equation will remain as constant while the daylight matrix will have a dimension of 145 by 2321 (145×16 sky patches + 1 ground patch).

The Three-phase method: accounting for variations in the window assembly layers

The BSDF data for a given window assembly is subordinate to the ray scattering properties of individual fenestration layers. Any alterations in a single fenestration layer impacts the ray scattering behavior of the entire window assembly necessitating the generation of a new BSDF data set accordingly. For example, considering a daylight interior space with a single clear-glass window utilizing venetian blinds as the shading device, the number of BSDF data sets that can be defined to account for the ray scattering behavior of the entire window system is driven by the applied variations in the state of the blind slats in the scene: if the state of the blind slats are changed from 15° to 60° , the ray scattering behavior of the venetian blinds as a fenestration layer changes as well. Consequently, with each permutation of a single state of shading devices and the constant optical properties of the glass layer, a separate BSDF data set must be generated to account for the ray scattering behavior of

the entire window assembly. The total number of the BSDF data sets incorporated in this simulation scene, depends on the number of shading states that the user decides to account for as part of the variables in the applied daylight control strategies in the space.

The Three-phase method: accounting for exterior obstructions

For a single sensor point within a given interior space that receives daylight through a single window assembly with no outside obstructions, it is sufficient to calculate a single Daylight Matrix to describe the relation between the contribution of each sky subdivision patch and the 145 incident ray patches on the glazing surface using the Klems' original subdivision scheme. However, if an outside obstruction in immediate adjacency with the glazing surface (for example, an overhang shading device on the building's facade) is present in the simulation scene, the applied ray sampling process conducted on random points across the entire glazing surface will not be sufficient

to accurately account for the impact of the exterior obstruction on the incident luminous flux. The reduced accuracy in the simulation results, is due to the fact that an identical number of patches (145) are referenced to describe a more complex daylight exposure/obstruction situation in comparison with the first case, where there is no outside obstructions in the scene.

Responding to the added complexity, it is suggested that the window glazing surface is subdivided into two or more segments so that a Daylight Matrix can be defined per individual segment. Therefore, an identical number of Klems' patches (145) can be used to describe the daylight exposure/obstructions relative to a smaller area of the glazing surface. The consequent higher "resolution" (as the ratio of the number of patches referenced for incident flux to the surface area referenced for ray sampling) results in higher accuracy in the simulation results accounting for the shading effect on the incidence of luminous flux. Another possible approach for greater accuracy in such scene

description is the application of Klems' coordinate system with greater number of subdivision patches (such as quadrupling each of 145 patches in the Klems' original scheme) to result higher resolution in the ray-sampling process for incident luminous flux.

The two simulation scene descriptions (with and without immediate outside obstruction) include only a single window assembly in the daylit space. If multiple windows are present in the same orientation, the calculation of a single daylight matrix per window can provide sufficient accuracy in the simulation results, if no immediate obstructions impact the windows' daylight exposure. On the other hand, the presence of exterior obstructions relative to a single window assembly (or more) requires further subdivision of the corresponding glazing surfaces. The required number of Daylight matrices and/or the subdivision scheme referenced for BSDF data in such simulation scenes is driven by any number of factors such as the variations in the exposure/obstruction conditions across the window assemblies, the time intervals during which the

exterior obstruction is present, the complexity of the consequent shading pattern, etc. It is suggested that the user should determine the level of accuracy that is considered as “sufficient” for a simulation run via the Three-phase method. There is not a single methodology that can be identified as a comprehensive solution that is applicable to all possible daylight exposure/obstruction situations in daylit spaces.

The Three-phase method: accounting for direct solar contributions

Using the Three-phase method, the daylight matrix is generated through sampling of all sky patches (145 patches utilizing the Tregenza’s sky subdivision model) per each Klem’s subdivision patch resulting a total number of 21,025 individual daylight coefficient values for a uniform white sky. The calculated daylight coefficients account for both direct daylight contributions (rays leaving a sky patch and directly hit a given Klem’s patch) and reflected daylight contributions (rays leaving a sky patch and hitting the

ground and/or other surfaces before hitting the target Klem's patch). Considering the simulation sky model that is developed for a given point in time using a local weather data file, the calculated location of the disk of the sun in the sky dome is interpolated to the three sky patches in the closest proximity of the real-world sun position in the Three-phase method. (Figure 13)

The direct daylight contributions (rays directly hitting a given Klem's patch) as part of the daylight coefficient matrix in the Three-phase method include rays leaving the four sky patches representing the sun as well as rays leaving all other 141 sky patches. Although such simulation of direct daylight contributions accounts for greater luminous flux values for rays leaving the three sky patches representing the sun (based on the generated sky model via point-in-time weather data) in comparison with the rays originated from the remaining 142 patches, the process of interpolating direct solar contributions to three adjacent sky patches diminishes the overall precision of the Three-phase simulation

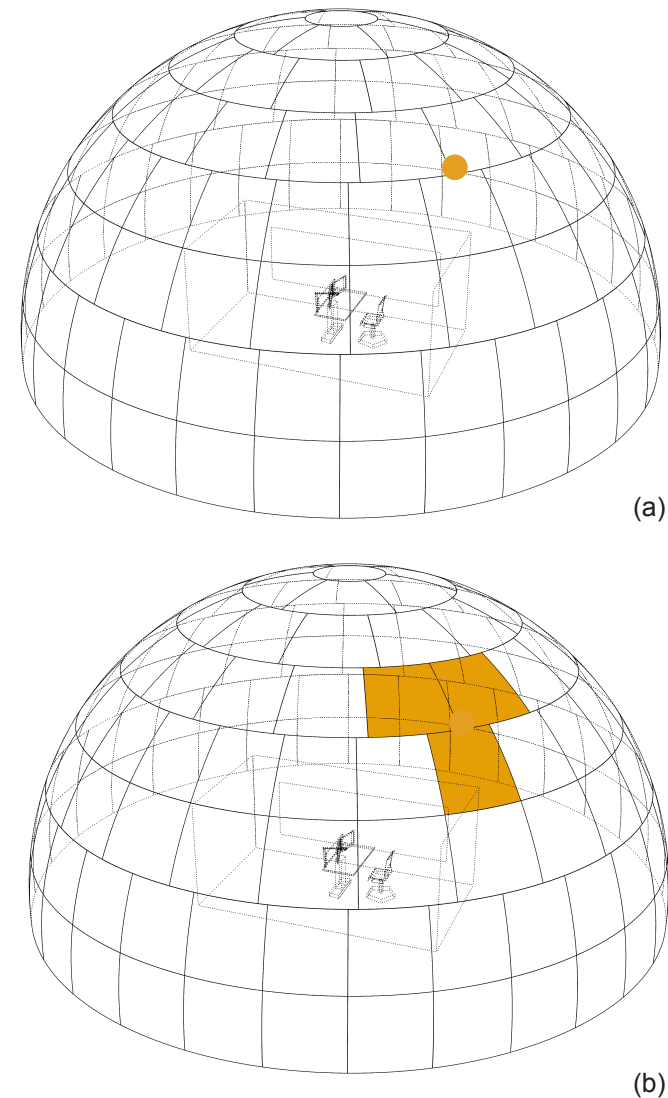


Figure 13: (a) the real-world position of the sun in the sky dome at a given point in time (b) three sky patches identified as the "sun" according to their proximity to the actual position of the sun in the sky dome

results at target sensor point(s) and/or the per-pixel luminance values at a given point of view.

The Three-phase method: uniform ray-scattering in response to incident direct solar patches

Using the Three-phase method, the geometric properties of a single fenestration assembly (such as its outline and orientation) is modeled via a single polygon (or a combination of connected polygons) as part of the digital 3D simulation scene. Considering the example of a clear-glass window assembly with venetian blinds as the shading devices, the calculated BSDF data for the whole assembly at a given shading state (such as 45° open slats) will be uniformly applied across the entire surface of the corresponding polygon(s). As a result, if a direct solar luminous flux hits a part of the glass layer from the outside, the simulated distribution of the flux at the interior space is not limited to the corresponding region of incidence on the fenestration polygon, but instead, it is uniformly attributed to the entire surface of the fenestration

polygon in the model. This level of generalization for the penetration of direct solar patch at the interior space will result in overestimated/underestimated predictions of daylight dynamics. It will hamper on the accuracy of the predicted illuminance values and/or luminance distribution patterns, glare indices, and solar heat gain values in the examined daylit space.

The Five-phase method (McNeil 2013) is developed to address the deficiency of precision in the Three-phase method simulation results with regards to direct solar contributions and the corresponding ray-scattering behavior by complex fenestration systems in response to the incident direct solar patches on the glazing system.

$$E = VTDS - VdTdS + CdsSds$$

E : Predicted illuminance/luminance value

V : View Matrix

T : Transmittance Matrix

D : Daylight Matrix

S : Sky matrix

Vd : Direct view matrix

T : Transmittance Matrix

Dd : Direct daylight matrix

Sds : sky matrix with direct sun only

Cds : direct sun coefficient matrix for a high-resolution matrix of sun positions

S_{sun}: matrix for a high-resolution sky description exclusive to sun positions and corresponding radiance values

Equation 12

2.5 The Five-phase Method:

The outcome of a daylight simulation using the Three-phase method represents the impact of both direct and indirect daylight contributions as a single illuminance value for a target sensor point or a single per pixel luminance value in a luminance distribution map. The Five-phase method introduces a methodology to segregate the direct solar contributions from the original Three-phase cumulative simulation result and replace it with a prediction of direct solar contributions with higher precision. The outcome of a Five-phase simulation, therefore, is comprised of the indirect daylight contributions by a Three-phase simulation and a high-precision prediction of the direct daylight contributions. The Five-phase method equation explicates this procedure. (Equation 12)

The first part of the equation (VTDS) relates to the cumulative simulation result using the Three-phase method. The second part of the equation (VdTdS) is the outcome of a Three-phase simulation that only

accounts for the direct daylight contributions. The third part of the equation ($CdsS_{sun}$) relates to the high-precision direct daylight contributions that is calculated to replace the Three-phase direct daylight contributions.

VTDS: Three-phase cumulative simulation result

The first part of the Five-phase equation is identical to the Three-phase equation as the product of view, transmittance, daylight and sky matrices on a point-in-time basis. The outcome of this matrix multiplication is a cumulative prediction of illuminance and/or luminance values based on the Three-phase method's calculation of both direct and indirect daylight contributions.

VdTDdS: Three-phase simulation of direct daylight contributions

The second part of the Five-phase equation is a Three-phase matrix multiplication procedure that unlike the

first part accounts for the direct daylight contributions exclusively. Similar to the daylight matrix referenced in the cumulative Three-phase simulation (first part of the equation), the direct daylight matrix utilizes the Tregenza sky subdivision model to discretize the sky dome into 145 patches. However, the direct daylight matrix only accounts for the daylight contribution by rays directly leaving a sky patch and hitting a given Klems' patch.

The Direct View Matrix, similar to the View Matrix referenced in the cumulative Three-phase simulation (first part of the equation), represents view coefficients using the Klems' coordinate system. Unlike the view matrix, the direct view matrix only accounts for rays passed through the fenestration system and directly hitting a Klem's patch on a sensor point. As a result, the contributions by rays passed through the fenestration system and reflected off the surrounding surfaces at the interior space before falling on a target sensor point are excluded in the direct view matrix. The

direct sky matrix that is referenced in the second part of equation uses the Tregenza sky subdivision.

CdsSds: High-precision direct daylight contributions

The third part of the equation uses a “high-resolution” sky description that is exclusive to the location of the disk of the sun in the sky dome. The advantage of this high-resolution sky model (in comparison to the Tregenza’s subdivision scheme utilized in the Three-phase direct sky description (second part of the equation)) is due to the application of Reinhart’s sky subdivision resolution resulting in 36 times greater number of patches. The Reinhart’s sky discretization model allows for subdividing a single Tregenza sky patch to a square matrix of patches with smaller solid angle and surface area (Equation 13).

Utilizing a 6 by 6 Reinhart subdivision matrix ($n = 6$), a single Tregenza patch (with the exception of the zenith) is subdivided into 36 smaller patches. As a result, a

$$d = (n^2 \times 144) + 1$$

d : total number of Reinhart's sky subdivision patches
*n*²: size of the square matrix of subdivision

Equation 13

$$\Omega = \frac{A}{r^2}$$

Ω : the solid angle of the sky dome
 A : the surface area of the sky dome
 r : the radius of the sky dome

$$\Omega_T = \frac{\Omega}{145}$$

Ω_T : the solid angle of a Tregenza sky patch

$$\Omega_R = \frac{\Omega}{d} = \frac{\Omega}{(n^2 \times 144) + 1}$$

Ω_R : the solid angle of a Reinhart sky patch

d : total number of Reinhart's sky patches
 n^2 : size of the square matrix of subdivision

for $n = 6$:

$$\Omega_R = \frac{\Omega}{(36 \times 144) + 1} = \frac{\Omega}{5185}$$

$$\frac{\Omega_R}{\Omega_T} = \frac{\frac{\Omega}{145}}{\frac{\Omega}{5185}} = \frac{5185}{145} = 35.758620$$

Equation14

total number of 5185 sky patches are referenced in the high-resolution sky model:

$$(36 \times 144) + 1 = 5185$$

With the exception of the zenith, the solid angle and the surface area of a single Reinhart sky patch is equal to the solid angle and the surface area of the Tregenza sky patch divided by the size of the Reinhart square matrix of subdivision (Equation 14)

In contrast to the interpolation process of the Three-phase direct solar calculations (part two of the equation), where the position of the sun is interpolated to the nearest three sky patches, the high-resolution sky model interpolates the calculated location of the sun in the sky dome to the center of a single sky patch in the closest proximity. As a result, a total number of 5,185 individual sun positions is calculated by locating a single sun at the center of each sky patch under Reinhart's sky subdivision scheme. (Figure 14)

The solid angle and the surface area of the entire sky dome is identical in both Tregenza and Reinhart sky subdivision models, yet, the availability of greater number of patches results in a higher resolution in the Reinhart's model (5185 sky patches where $n=6$) in comparison to the Tregenza's model (145 sky patches).

The direct solar coefficient matrix in the third part of the Five-phase method equation includes daylight contribution values per disk of the sun in the high-resolution sky description relative to a given sensor point or point of view. Using the local weather data file, the actual location of the disk of the sun in real world is calculated. For every hour across an entire year, the high-resolution sky matrix of sun positions is referenced to identify a single sun position (out of 5,185 positions) that is in closest proximity to the calculated location of the disk of the sun in real world at a given point in time (Figure 15).

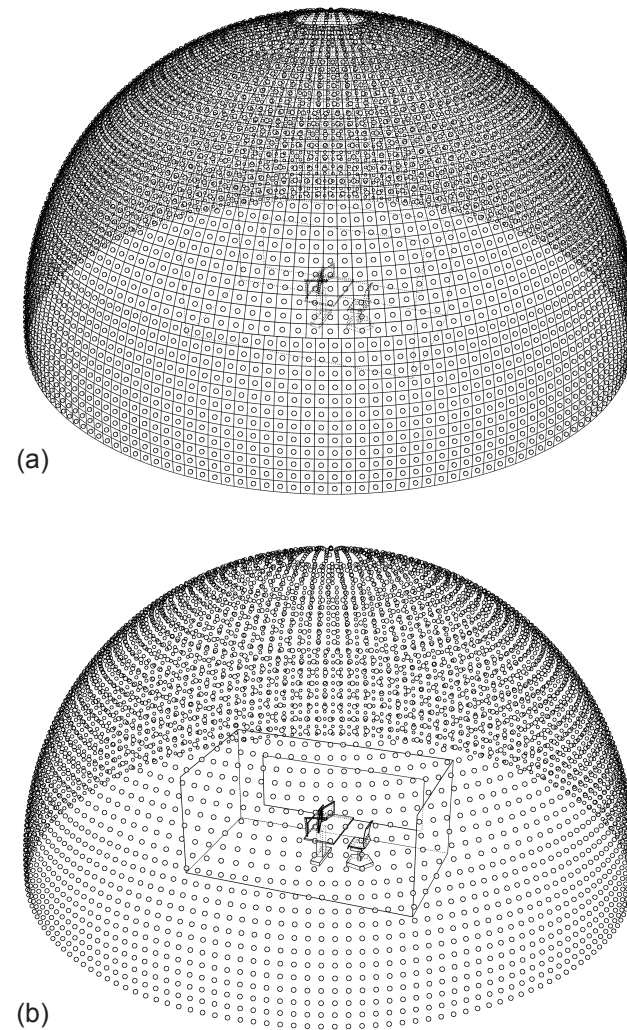
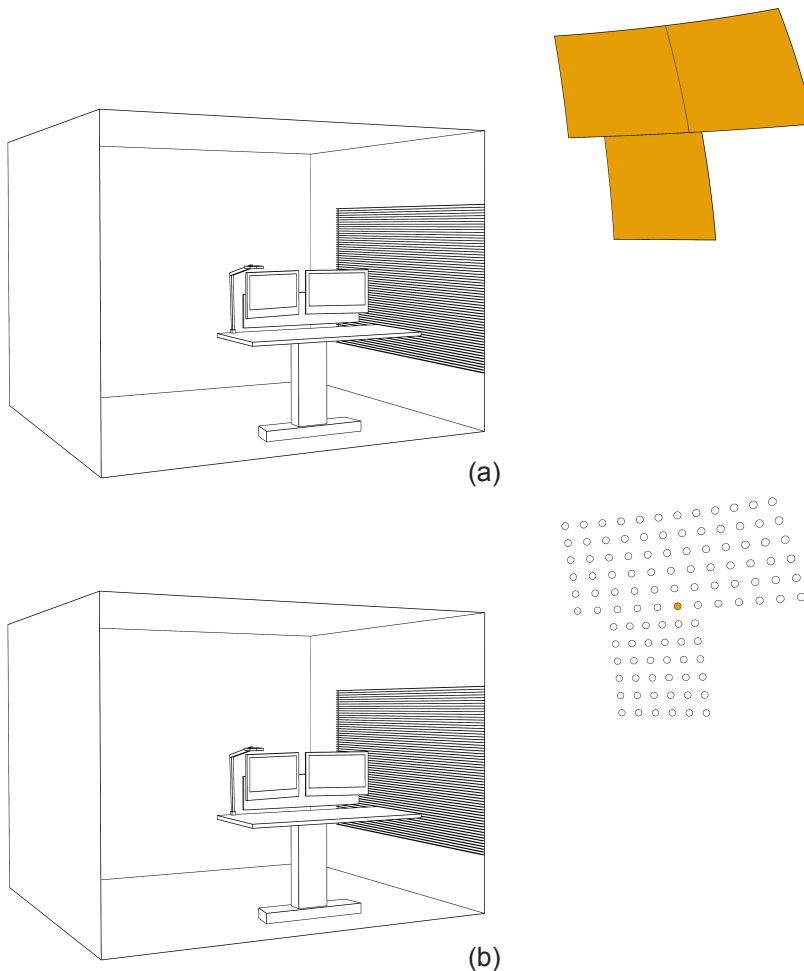


Figure 14: (a) a total number of 5,185 individual sun positions is calculated by locating a single sun at the center of each sky patch under Reinhart's sky subdivision scheme (b) the high-resolution sky dome exclusive to sun positions



A total number of 8760 sky matrices are generated to specify the location of the disk of the sun in the sky dome and the corresponding luminance value based on the hourly weather data file.

The multiplication of the direct solar coefficient matrix and the hourly sky description matrices for solar contributions provides the illuminance and/or luminance values for the direct solar contributions at the target sensor point(s) or point of view. The high-precision prediction of direct daylight contributions replaces its counterpart in the Three-phase prediction of direct daylight contributions (part two of the equation). The outcome of a daylight simulation using the Five-phase method, therefore, is a more accurate prediction of daylight distribution that incorporates the ray-scattering behavior of complex fenestration systems for both indirect and direct daylight contributions.

Figure 15: (a) using the Tregenza sky subdivision model in the Three-phase method, the position of the sun is interpolated to the nearest three sky patches (b) the high-resolution sky model interpolates the calculated location of the sun in the sky dome to a single sun disk position

Chapter 3
Research Methodology

Research Methodology

This chapter describes the simulation workflow in detail. Although the workflow closely follows the Three-phase and the Five-phase documents (McNeil 2013) the procedures are explained here inside out. The motivation is two folds: i) to provide a clear explanation of the complex processes (which improves the accessibility of a highly technical simulation technique to a larger audience, particularly architects and other building professionals who perform lighting simulations as part of their practice) and ii) to provide a transparent workflow that can be replicated for users who may not be familiar with the Three phase and Five Phase methodologies.

3.1 Preparation of the simulation scene:

A digital 3D model for a south-facing shared office space is developed as part of a high-rise development in Downtown Seattle (Figure 16). The model includes

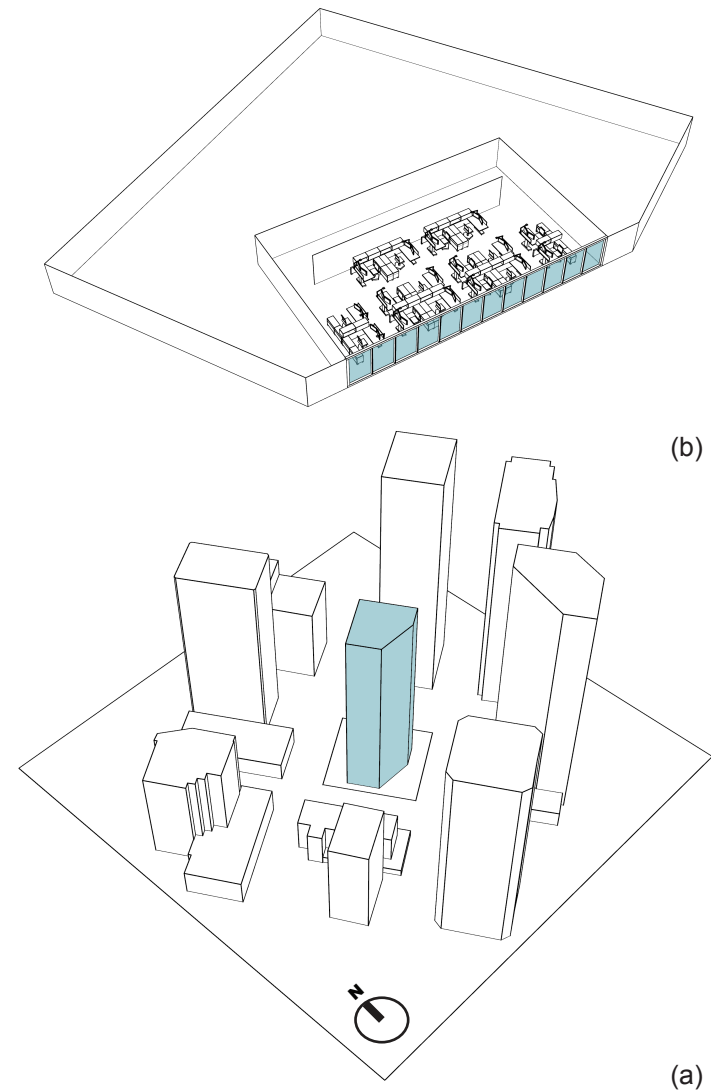


Figure 16: (a) the high-rise office building in the simulation model (b) the shared office space developed as the simulation scene. The high-lighted shows the glazing surface areas oriented due south.

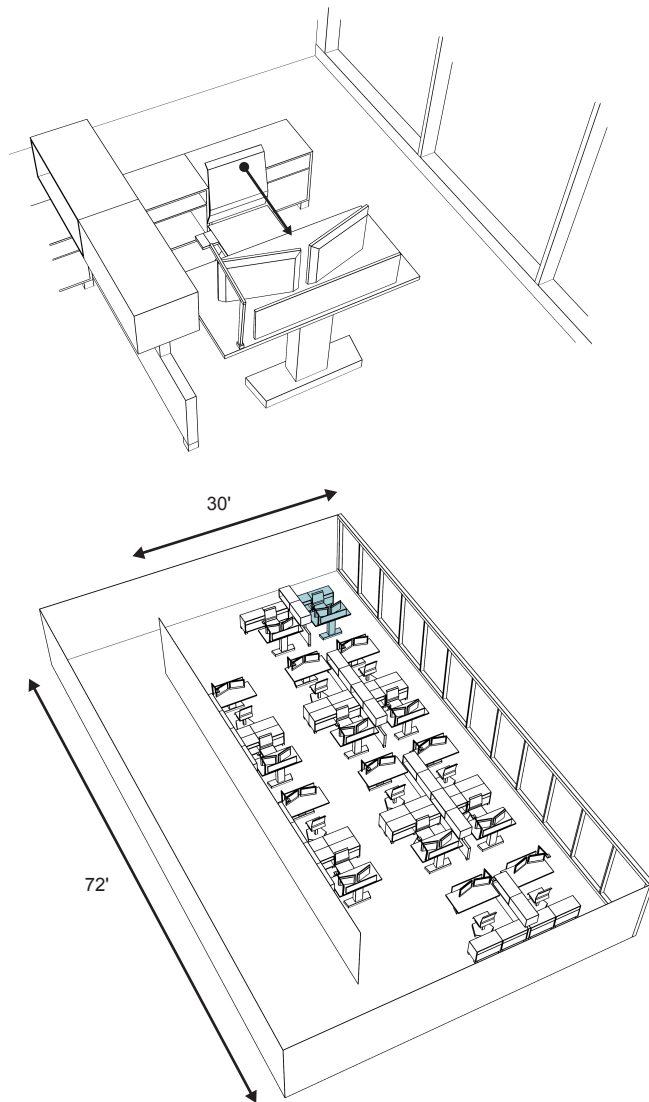


Figure 17: The 3D model of the shared office space. The high-lighted shows the selected workstation for the simulation of luminance distribution maps at the target occupant's point of view.

a total number of 16 workstation units situated in parallel to the fenestration system. The 3D geometry of the adjacent building context is included to simulate the impact of outside obstructions on the distribution of daylight in the interior spaces. (Figure 17)

The 3d geometry is imported to Radiance through the DIVA-for-Rhino plug-in (Jakubiec and Reinhart 2011). The 3D geometries in the simulation scene are distributed in Rhino object layers so that all geometries in a given layer are assigned to an identical Radiance material definition.

Material Definition in Radiance:

Depending on the target daylit scene, a variety of material definitions can be selected to model the optical properties of different object surfaces in response to incident light rays. Any Radiance material definition requires the specification of an “id” attribute referring to which, a given material definition is distinguished from another material definition. The

structure of a Radiance material definition as a particular sequence of lines and words and attributes in plain text format is defined by the material type. A total number of 25 separate material types are provided in Radiance allowing for simulating a specific optical property and visual appearance relative to object surfaces in the scene. The structure of four primary material types used in this project are as follows:

Plastic:

mod plastic id

0

0

5 red green blue spec rough

The “red”, “green” and “blue” attributes relate to the RGB channels defining the surface reflectance (and color). The “spec” and “rough” attributes define the specularity and roughness of the object surface, respectively. An example of a plastic material definition that is used in the simulation scene is as follows:

```
void plastic wall_mat  
0  
0  
5 .5 .5 .5 0 0
```

The “wall_mat” is the string argument for the “id” attribute. This material is assigned to the interior wall surfaces in the simulation scene resulting a 50% reflectance (red=0.5, green=0.5, blue=0.5). The material has no specularly or roughness (spec=0, rough=0).

```
Glass:  
mod glass id  
0  
0  
3 rtn gtn btn
```

The “glass” material type is considered as transparent. The “rtn”, “gtn” and “btn” attributes regulate the RGB channels for the transmissivity of the glass. The glass

material type assigned to the glazing surfaces in the simulation scene is defined as follows:

```
void glass glazing
```

```
0
```

```
0
```

```
3 0.73 0.73 0.73
```

This glass material definition results in a 73% transmissivity of the glazing surfaces.

```
BSDF
```

```
mod BSDF id
```

```
6+ thick BSDFfile ux uy uz .
```

```
0
```

```
0
```

The “thick” attribute refers to the thickness of the fenestration assembly for which the BSDF data is referenced. The “BSDFfile” refers to the name of the BSDF file in “.xml” format. The “ux, uy, uz” attributes to

the normal vector of ground plane (the world +Z axis in Rhino).

Glow

mod glow id

0

0

4 red green blue maxrad

The assignment of a “glow” material to an object surface results in emission of light from front side of the object surface. The “red”, “green” and “blue” attributes define the RGB channels that specify the color of emitted light. The “maxrad” refers to “maximum radius for shadow testing”. An example of a glow material that is used in simulation scene to represent the luminous computer screen surfaces is as follows:

void glow 250cdm2_screen

0

0

4 1.39 1.39 1.39 0

The 1.39 argument passed for the red, green and blue attributes results in a uniform light emitting surface where the luminance value across the entire surface is equal to 250 cd/m^2 .

Object Files in Radiance:

The object layers in the Rhino model consist of surfaces defined as NURBS geometry. Exporting the NURBS geometry from Rhino to Radiance, each individual NURBS surface is transformed into a Radiance polygon (or a combination of Radiance polygons) defined by vertices in three dimensional space. Depending on the complexity of a simulation model, the number of Radiance polygons that define the three-dimensional properties of a physical object in the simulation scene can vary from a few quadrilateral polygons defining the walls, floor and ceiling surfaces of a shoe-box model to a combination of thousands of multi-lateral polygons corresponding with a workstation unit object. The exported geometry from Rhino are saved as separate Radiance objects files in “.rad” format. A polygon primitive in Radiance is defined as follows:

mod polygon id

0

0

3n

x1 y1 z1

x2 y2 z2

...

xn yn zn

The “mod” attribute refers to the “id” attribute of the material definition as the Radiance modifier assigned to the polygon. As a result, the optical properties of the material matching the given unique id will be assigned to all the corresponding polygons. Considering Radiance polygons are defined by vertices (points) in three-dimensional space, a minimum of 3 vertices must be provided to define a single planar surface. As a result, the total number of vertices in a given polygon definition is a product of 3. The “id” attribute of the polygon definition allows for distinguishing a single polygon from all other polygons (even with the same modifier) in a Radiance object file. Using DIVA-for-

Rhino to transform objects in the Rhino simulation scene into Radiance polygon definitions, the “id” attribute for a set of polygons with an identical modifier (material definition) is set to a concatenation of the string relative to the modifier id (material name) followed by an integer representing the polygons’ index number. An example of a consequent Radiance object file for the workstation units in the simulation model is provided.

Organizing the exported objects in the simulation scene:

The consequent polygon definitions by exporting the simulation scene from the 3D modeling environment of Rhino to Radiance must be organized so that a target set of polygons can be independently assembled and passed for a single Radiance program call.

A common approach for such organization of exported geometry is to segregate a set of polygon definitions relative to a given physical object in the simulation scene, such as a workstation unit, and save the set as an individual Radiance file in “.rad” format. Such classification of polygon definitions based on the corresponding object can be extended to segregating polygons that define a particular component of an object, such as the countertop as part of a furniture unit, and saving each object component set as a separate Radiance file.

Another common approach in organizing the exported geometry is to segregate polygon definitions based on

their corresponding modifier so that a set of Radiance polygons with an identical material definition, such as all surfaces in the simulation scene described as stainless steel, can be saved in a separate file.

Depending on the user preferences, the complexity of the simulation scene and the simulation scope, a combination of both approaches can be utilized to organize the exported polygon definitions as separate Radiance object files.

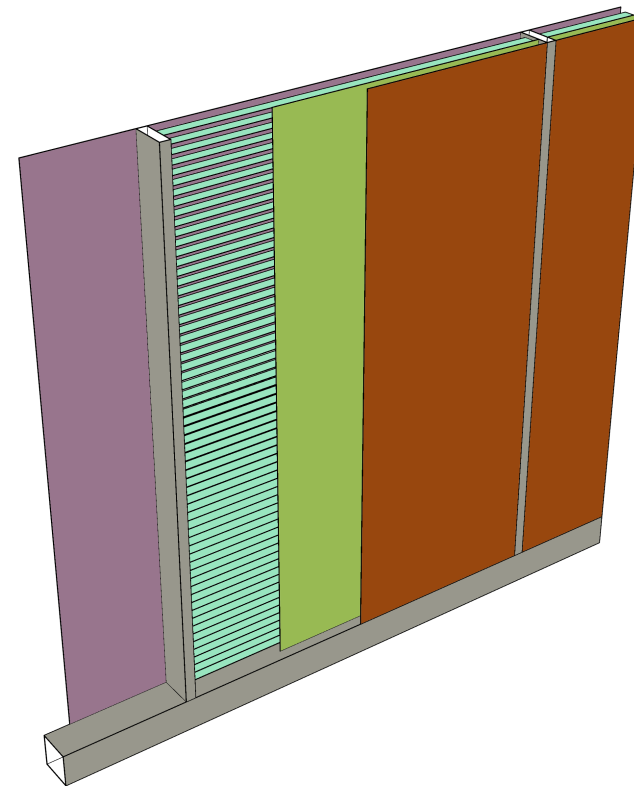
**Daylight, Transmission and View Matrices:
referenced surface areas for the ray-sampling
processes**

The simulation model includes three set of planar surface objects that are referenced as part of the ray-sampling process: the daylight, the transmission and view matrix surfaces.

The daylight matrix surface is modeled as co-planar with the outermost side of the window frame so that any given point on the daylight matrix surface

(including points on its perimeter) can see the surrounding outside environment without any obstructions from the window frame. Given that the fenestration system in the studied simulation model consists of 11 glazing panes separated by the window frame, there are 11 daylight matrix surfaces with two-dimensional geometric layouts as identical to those of the glazing panes. (Figure 18)

The view matrix surface, on the other hand, is modeled as co-planar with the innermost side of the window frame so that any given point on the view matrix surface can see the interiors without any obstructions from the window frame. The three-dimensional geometric properties of the transmission matrix surface is modeled as identical to those of the view matrix surface. Using Radiance, a reference to two surface polygons coincident on a shared plane in the same simulation call results in excluding one surface from the ray-tracing process. In this case, however, the definition of the view and transmission matrix surfaces as identical polygons situated on a shared plane does



- Daylight Matrix Surface (daymtxsurf.rad)
- Glazing (glazing.rad)
- Venetian Blinds (venetianblind.rad)
- View Matrix Surface (viewmtxsurf.rad) & Glazing_BSDF (glazing_bsdf.rad)

Figure 18: the fenestration assembly in the 3D simulation model

not result in excluding either surface from the simulation process as each polygon is passed to a separate ray-sampling call. Similar to the daylight matrix surfaces, the two-dimensional geometric layout of the view and transmission matrix surfaces are also defined as identical to those of the 11 glazing panes.

Radiance genBSDF: generating the BSDF data for the fenestration system

The fenestration system in the simulation model consists of 11 identical glazing panes that are separated by the window frame. The venetian blinds span through the width of the each glazing pane and are distributed along the window height so that that the difference between the elevations of each two consecutive blind slat is 4 centimeters.

Using Radiance genBSDF program (McNeil et al. 2013; McNeil 2015), it is possible to compute the ray-scattering behavior of a specific fenestration assembly system and save the consequent BSDF data in “.xml” format. Since all 11 window frames in the simulation

model have identical glazing panes and the venetian blinds (as the shading component of the fenestration system), it is sufficient to compute the ray scattering properties of one of the 11 window frames and attribute the consequent BSDF data to the remaining 10 windows.

Using genBSDF, it is possible to compute the BSDF properties of a complex fenestration system following two approaches: i) including the window frame in the Radiance object files as an input to the genBSDF command. This approach is applicable to simulation scenes where the exact layout of the window frames is determined. ii) Excluding the window frame from the genBSDF call and considering the assembly components of the complex fenestration system (glazing surface(s), shading device(s), etc.) as infinite geometric constructs (in terms of the window height and width). In this approach, the ray-tracing process by the genBSDF call is only applied to a portion of the window as a sample of all fenestration system layers (glazing, blinds, etc.) representing its complex ray-

scattering optical properties. The benefit of this approach is that the generated BSDF data can be referenced to study the impact of the fenestration systems' BSDF properties on the daylight distribution at the interiors without having to determine a specific layout for the window frames.

The reason for pursuing either approach is to avoid the discrepancy caused by the window frame's inner edge during the BSDF computation : if the window frame is not included in the object files passed to the genBSDF call and the ray-sampling process is conducted for the entire span of fenestration assembly's width and height, the sampling points situated at the edge conditions (the perimeter of the assembly layout) will result in greater transmission of light to be accounted for in the output BSDF data. Such "light-leak" condition at the window edges, therefore, is avoided using either sampling approach in a genBSDF call.

Object files passed to the genBSDF call:

The 3D model for a single window assembly including the frame, glazing surface and the venetian blinds is saved as a separate Rhino 3D model and exported to Radiance as a set of object files in “.rad” format. The window 3D model is oriented so that the glazing surface’s normal vector pointed towards the interior side is parallel to the $-Z$ axis in the Rhino’s 3D editing environment. As a result, the glazing plane of the fenestration model is situated as parallel to the Rhino’s world XY plane. It is important to ensure that the entire fenestration model is situated below the XY plane where the Z coordinate of any given point on the model will be less than 0. (Figure 19)

The described changes in the orientation of the window assembly model is specific to the genBSDF calculation (resulting in a modification of the original orientation of the window assemblies in the simulation scene). The purpose for the modification is to maintain consistency with the three-dimensional coordinates system defined

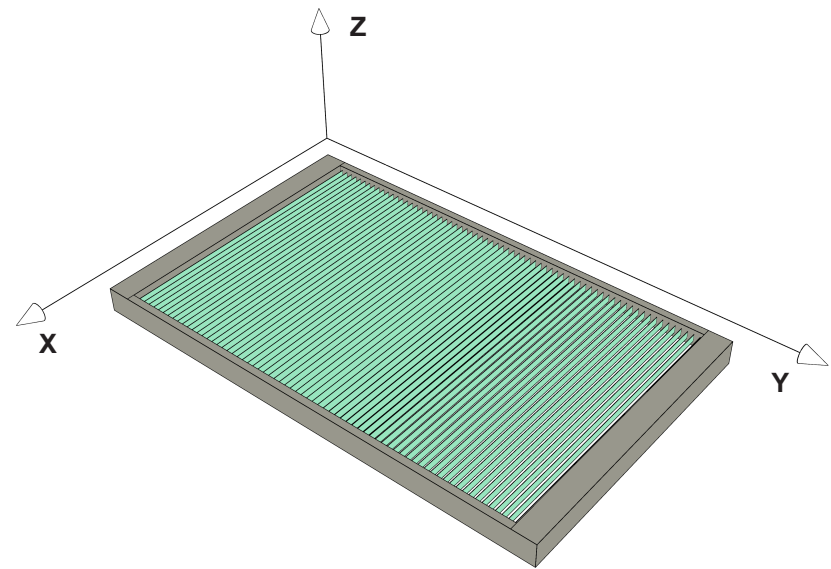


Figure 19: the fenestration geometry referenced in the genBSDF call

in the Lawrence Berkeley National Laboratory's (LBNL) Window software (LBNL 2013) in the Window software, the 3D coordinates system is defined so that the XY plane is parallel to the fenestration's glazing plane where the X axis runs across the width of the glazing and the Y axis spans along the glazing's height. The +Z axis in the Window coordinate system is defined as perpendicular to the glazing plane looking towards the interior side of the fenestration system.

The Radiance genBSDF program is developed so that the reference to ray directional properties as part of the ray-tracing process is based on such re-orientation of the window assembly model. As a result, it is possible to pass only a single fenestration layer, such as the venetian blinds, to the genBSDF call and use the consequent BSDF data in the Window software as part of another BSDF calculations for a customized combination of individual assembly layers.

BSDF data: variable resolution and constant resolution

The genBSDF program allows for generating two types of BSDF data for a given fenestration assembly model: constant resolution and variable resolution.

The constant resolution BSDF is generated based on the Klems' original subdivision scheme resulting 21025 individual transmission coefficients where a single coefficient is the luminous intensity multiplier for the transmitted ray relative to the luminous intensity of the original incident ray. The index number of a given transmission coefficient at a given line number corresponds with the Klems' incident and transmission directional patch numbers respectively. Using the Klems' original subdivision scheme, therefore, results in a constant number of coefficients to be computed by genBSDF.

The variable-resolution BSDF data, on the other hand, is not based on the Klems' directional subdivision basis. Instead, it allows for increasing the number of

directional subdivisions according to the density of transmitted/reflected rays in a particular direction driven by the ray-scattering behavior of the specular object. This variable-resolution description of ray-scattering properties is referred to as Tensor Tree BSDF data.

Using the constant resolution model, it is possible to uniformly subdivide each Klems' patch into smaller patches to increase the total resolution of the Klems' model. However, such uniform increase in the resolution will result in allocation of processing time for computing transmission/reflection coefficients with insignificant contributions to the overall precision of the BSDF data due to the little intensity of predicted transmitted/reflected rays at the respective three-dimensional directions.

On the other hand, considering the inherent issue with the Three-phase method to account for direct solar contributions in the final luminance distribution results, the Klems' original subdivision scheme is identified

with adequate resolution to account for the ray-scattering properties of the complex fenestration system in the simulation scene for non-direct solar contributions. As a result, the constant resolution BSDF model is referenced in the genBSDF call to be used as the transmission matrix in the Three-phase part of the simulation process.

A variable-resolution Tensor Tree file is also generated using a second call to genBSDF with the same window assembly object files and the output Tensor Tree BSDF data file is referenced in the high-resolution direct solar component of the Five-phase simulation process.

Radiance View Definition:

The perspective view in the Rhino 3D modeling environment is setup according to the occupant's viewpoint at the selected workstation unit. Exporting the simulation scene to Radiance, the Rhino perspective view is exported as a Radiance view file in

“.vf” format. Accounting for human eye’s view range for visual comfort studies, Radiance view specification options are added to the view file to define a hemispherical fisheye view ($180^\circ \times 180^\circ$) at the examined occupant’s point of view.

Radiance Uniform White Sky:

Two concentric identical hemispheres are modeled using Radiance as symmetrical relative to the ground plane. A glow material is applied to the surface of both hemispheres resulting two white hemispheres emitting light uniformly across their surface area. The hemisphere situated above the ground plane represents the sky dome while the other hemisphere is designed to account for the contributions by the reflected light off the ground. Both Radiance hemisphere definitions along with the white glow material as the respective modifiers are saved in a single “.rad” file.

3.2 The Three-phase Simulation Process:

The first part of the Five-phase equation is the outcome of a Three-phase simulation process. As described in the previous chapter, three matrices of coefficients must be developed to describe the luminous flux transfer from the sky to a given sensor point (for predicting illuminance values) or on a surface within the target viewpoint for predicting luminance distribution.

Radiance Octree Files: describing the simulation scene

An “octree” file in Radiance incorporates the objects and the material definitions in a simulation scene. An octree file, therefore, can be passed to other Radiance programs as the description of the simulation scene by referencing the directory path where each individual object/material file is saved. The Radiance “Oconv” program generates octree files by receiving the target

simulation scene's object files (in ".rad" format) as well as the material definition files (in ".mat" format). Typically, all the object/material files are located in the same project directory. The user can choose to save these files in sub-directories of the project folder (highly recommended) for the purpose of organizing the entire simulation project files.

By default, the octree file generated by an oconv call stores the directory information for each file as relative paths within the project folder. As a result, any changes to the location of files referenced in an octree file will cause errors in the simulation process as the respective relative paths are no longer valid. Alternatively, it might be desirable to have an octree file that contains the entire content of the object/material files describing the simulation scene instead of exclusively referencing to the directory path at which these files are saved. The oconv program allows for generating such cumulative octree files by providing a "freeze" option as part of the command call. In this simulation project, however, the default setting for the

oconv call is used so that the consequent octree file references the simulation scenes' object/material file names and the respective directory paths only.

The octree file for the Three-phase part of the simulation is generated by passing the exported simulation scene object files (including the daylight and view matrix surface object files) as well as the project's material definition file. The outcome octree files is saved as "model_3ph.oct" is a project folder's sub-directory names as "octs".

Three-phase simulation process: the view matrix

The defined view parameters along with the dimensions of the final luminance distribution map in the format of a High Dynamic Range (HDR) image are passed to the Radiance's "vwrays" program. The vwrays call allows for tracing all sample rays used in the rendering of a scene with an origin of departure set to each individual pixel of the final HDR image. As a result, for an output HDR image set to 1000 pixels on

both x and y sides, a total number of one million (10^6) ray origins are referenced in the ray-sampling process.

The computed ray property data via the `vwrays` call (per individual pixel) is passed to the Radiance's "rcontrib" program. The `rcontrib` program allows for segregating the individual light sources in a given Radiance scene description and computing the contribution by each light source to the overall natural/artificial light distributions. The mathematical model for the Klems' subdivision scheme is also passed to the `rcontrib` in the format of a Radiance ".cal" file. The Three-phase octree file is another component passed the `rcontrib` call as the description of the simulation scene's object surfaces and the respective material definitions.

The `rcontrib` call requires the specification of the target light source in the scene for which the contributions should be calculated per sensor point or pixel at the point of view. The view matrix describes the contribution of transmitted light through the window on

surfaces within the target viewpoint. The “viewsurf” (as the name of the Radiance modifier (material name)) is assigned to the view matrix surface polygon and passed to the rcontrib call. The output of the rcontrib call is set as individual images with identical dimensions that were referenced in the vwrays call. The output images are saved in a project folder’s sub-directory named as “viewpics”.

The described rcontrib call computes the contributions by a uniform glow surface (view matrix surface) at the innermost layer of the fenestration system to the interior scene. Since the Klems’ subdivision scheme is referenced in this process, the rcontrib computes the contributions as if each Klems’ patch on the glow surface is the only source of light in the scene. Therefore, a total number of 145 HDR images are generated at which the distribution of luminance values in the occupant’s point of view is predicted as a result of contributions by a single Klem’s patch assigned with the “viewsurf” glow material. These 145 HDR images

are the view matrix component in the Three-phase simulation for luminance distribution maps.

Three-phase simulation process: the daylight matrix

In the simulation process of the Three-phase view matrix, the `vwrays` program is called to determine the sample rays' origin of departure as the directional properties are passed to the `rcontrib` call. The Radiance `genklemsamp` program plays the same role in the Three-phase daylight matrix simulation process. Unlike the `vwrays`, the `genklemsamp` determines the origin of departure for sample rays on a target polygon surface. Considering the daylight matrix contains coefficients that relate the radiance of individual sky patches to the corresponding incident luminous flux on the exterior side of the fenestration system, the "daymtxsurf.rad" object file is passed to the `genklemsamp` call on which the origin of sample rays is situated. The `genklemsamp`, by default, uses the Klems' directional subdivision model. The data

describing the sample ray properties (as the outcome of the `genklemsamp` call) is passed to the `rcontrib` program. The mathematical model as a Radiance file in “.cal” format describing the Reinhart’s sky dome subdivision is another input for `rcontrib`. The desired resolution for Reinhart’s sky subdivision model can be specified using the Radiance’s “MF:(n)” option where (n) is the size of the Reinhart’s square matrix of sky patch subdivision. Additionally, the Radiance modifier assigned for the uniform white sky dome named as “sky_glow” is specified in the `rcontrib` call so that the contributions by each individual sky patch (as an independent light source) can be calculated. Similar to the simulation process for the Three-phase view matrix, the ““model_3ph.oct” octree file is passed to the `rcontrib`.

The result of described `rcontrib` call is the Three-phase daylight matrix saved as “daylightmatrix.dmx” in a project folder’s sub-directory names as “matrices”.

The Three-phase Simulation Process: The Transmission Matrix

As described in the previous section, the transmission matrix containing the BSDF data based on the Klems' original subdivision model is calculated using the genBSDF program. The consequent Klems-based BSDF data is saved as "fullwindow_klems.xml" in a project folder's sub-directory named as "BSDF".

3.3 The Three-phase Direct Solar Component

The second part of the Five-phase equation is the direct solar component of in the Three-phase simulation process. The direct daylight and view matrices are calculated for this part of the Five-phase simulation process as follows:

Three-phase Direct Solar Component: direct daylight matrix

The direct daylight matrix contains coefficients relating the radiance of the sky patches and the direct incident rays (rays with no previous inter-reflections with the surrounding context) on the exterior side of the fenestration system.

Avoiding inter-reflection by the object surfaces in outside context, the Radiance ray-tracing option specifying the number of ray ambient bounces is set to 0 (-ab 0). In addition, given the nature of ray-scattering

behavior by specular objects, the presence of a hypothetical set of surfaces in the outside context of the simulation scene (such as the adjacent building facades) with assigned material properties where the given value for the “specularity” attribute is greater than 0 ($\text{spec} > 0$) and the value assigned to the “roughness” attribute is less than 0.002 ($\text{rough} < 0.002$) results in mirror-alike reflection of the incident rays. Preventing the occurrence of such undesired specular reflectivity, the assigned Radiance modifiers to all objects in the simulation scene are replaced with a single modifier as a material definition for a plastic surface with black color ($R=0, G=0, B=0$) and no specularity or roughness ($\text{spec}=0, \text{rough}=0$).

The described changes in the assigned object surface modifiers is executed using the Radiance “xform” program. The modifier option (-m) in the xform call allows for specifying the name of the target modifier replacing the existing ones in the scene. All object files referenced in the Three-phase octree file are passed to the xform call. The transformed object surfaces with

the “black” modifier is passed to a new oconv call so that a new octree file named as “model_allblack.oct” for the entire simulation scene with black surfaces is generated. Since the definition for the “black” modifier is saved in the “my_room.mat”, it is necessary to include this material definition file in the new octree file as well.

The new octree file describing an “all-black” simulation scene is passed to an rcontrib call where the number of ambient bounces is set to 0 (-ab 0). All other command options for the genklemsamp and rcontrib calls in the direct daylight matrix computation is identical to those of the daylight matrix simulation process.

Three-phase Direct Solar Component: direct view matrix

The direct view matrix relates the incident rays transmitted through the fenestration and directly falling on simulation scene’s object surfaces at the interiors

(for luminance distribution predictions) or on a target sensor point for illuminance predictions.

The simulation process for the direct view matrix calculations is similar to the computational procedure pursued in the Three-phase view matrix calculations. The difference between the two simulation procedures is the number of ambient bounces specified, where in the direct view matrix calculations, the number of ambient bounces is set to 1 (-ab 1).

Three-phase Direct Solar Component: transmission matrix

The ray-scattering behavior of the complex fenestration system is described as a separate luminous flux transfer matrix that is independent from the daylight and view matrices. Therefore, the same transmission matrix used in the Three-phase simulation can be referenced in the Three-phase direct solar component calculations.

3.4 Simulation of high-precision direct solar contributions

The third part of the Five-phase method's equation is the simulation of the high-precision direct solar component.

Creating high-resolution sky description with 5185 sun positions:

The simulation of the disk of the sun as a Radiance polygon surface assigned with a "light" material does not yield the desired simulation results given the actual distance of the sun from the earth in comparison with the relative proximity of all other object surfaces in the simulation scene. A separate Radiance primitive, therefore, is available in order to specifically simulate light sources in significant distance from the actual simulation scene, such as the disk of the sun itself. This Radiance primitive named as "source" defines distant light sources according to the solid angle through which they are seen and their respective directional

vector. The structure of a Radiance “source” primitive definition is provided as follows.

```
mod source id
0
0
4 xdir ydir zdir angle
```

A Radiance “light” material definition corresponding with the radiance of the sun is also specified.

```
mod light id
0
0
3 red green blue
```

The light material definition is assigned an identifier (a name) as “solar” and saved as “suns.rad” in a project folder’s sub-directory titled “skies”.

Considering the required parameters in the definition of Radiance “source” primitive, the directional vector for

each sun position in the high-resolution sky must be provided. The Radiance “reinsrc.cal” file contains the mathematical model based on which the Reinhart’s sky patch directions for a given subdivision scheme can be calculated. Considering the 5185 sun positions are situated at the center of individual Reinhart sky patches, utilizing the reinsrc.cal mathematical model results in the three-dimensional coordinates of the directional vectors (“xdir”, “ydir”, “zdir”) as required parameters in a “source” primitive definition. Another required parameter in the definition of sun disks, is the solid angle for which, a constant value of 0.533 is determined for all sun positions. The outcome is 5185 individual sun disks that are defined as Radiance “source” primitives and assigned with the “solar” modifier.

The described simulation procedure is exercised via a Radiance “rcalc” call. The rcalc program, receives a set of data (records) from a specified resource and re-organizes the data based on a new layout in the output file. In this part of the simulation, the reinsrc.cal file

determines the data for the (x), (y) and (z) coordinates of directional vectors for a (6x6) subdivision scheme (MF:6); and this information is passed to the rcalc program. The target data layout in the output file is also passed to rcalc according to the definition format for a “source” primitive. The rcalc reads the (x), (y) and (z) coordinates for the directional vectors and replaces each (x), (y) and (z) triple set relative to a single sun position in a “source” primitive template named “sun”. The resultant 5185 sun positions in the format of Radiance “source” primitives are saved in the “suns.rad” file.

Creating new octree files:

To reach a high-precision prediction of direct solar contributions accounting for the BSDF properties of the fenestration system, the octree file generated in the Three-phase part of the simulation is not useful. In the Three-phase octree file, the venetian blinds object file is not included due to the Three-phase method’s low-precision prediction of direct solar component and the

respective ray-scattering and shadow pattern by the venetian blinds. In the third part of the Five-phase method simulation, however, a new octree file named as “model_suns.oct” is generated including the venetian blinds object file as well as the BSDF proxy object and the sky description for 5185 sun positions. Considering the direct solar contributions are targeted, all object surfaces are assigned with the “black” modifier (similar to the material transformation in the Three-phase direct daylight component) in the “model_suns.oct” file. In addition, a second octree is generated and saved as “model_nosuns.oct” using an identical procedure with the exception of excluding the suns.rad file.

The target occupant’s viewpoint properties along with the dimensions of the output luminance distribution image is passed to a vwrays call. The output of the vwrays call as sample ray origins and their respective directional properties is passed to a Radiance “rtrace” call. The rtrace call also receives the “model_nosuns.oct” file and calculates the first point of

incidence ($\cos \theta$) between a sample ray and a surface in the simulation scene along with the corresponding surface's normal vector. The output of the `rtrace` call is subsequently passed to the `rcontrib`. The `rcontrib` identifies each sun disk as an independent light source and computes their respective direct contributions to the simulation scene. The outcome of this `rcontrib` call is 5185 illuminance distribution maps in the format of HDR images. The resultant 5185 illuminance distribution maps are multiplied by a data distribution map in the format of a 1000 by 1000 pixel image where each pixel represents the outcome of material reflectance divided by π .

Three-phase Sky Description Matrix:

The EnergyPlus weather data file (.epw format) for a Typical Meteorological Year (TMY) in Seattle is used. Using DAYSIM's (Reinhart 2001) "epw2wea" program, the direct normal and diffuse horizontal irradiance values per hour across an entire year (365 days) is extracted from the ".epw" file and saved in a new file in ".wea" format. A single weather data line in a ".wea" format contains 5 values: the first three values correspond with the month, day and hour (0-23) and the last two values correspond with the direct normal and diffuse horizontal irradiance values, respectively.

The consequent weather data file saved as "seattle.wea" is passed to a Radiance "gendaymtx" call. The gendaymtx program generates a sky description using Perez (Perez, Seals, Michalsky 1993) all-weather sky model based on the hourly data for direct normal and diffuse horizontal irradiance values. By default, the gendaymtx refers to a Tregenza sky subdivision scheme to calculate the RGB values of

a sky patch at a single point in time. Considering the number of hours across 365 days, a total number of 8760 set of RGB values for each sky patch is calculated. By default, the output of a `gendaymtx` call is saved as an ASCII file where the first 8760 lines (excluding the file header) contain the hourly R, G and B values for patch #0 (the ground). The RGB values for patch #1 (the first patch in the Tregenza subdivision model) are distributed in the next 8760 lines. A blank line separates each two consecutive set of sky patch RGB data.

Accelerating the computational process, the output of the `gendaymtx` call, in this part of the simulation, is specified as binary float, instead of the ASCII format, by passing the `(-of)` option. The resultant annual sky description matrix (the matrix rows correspond with the patch index and the matrix column corresponds with the R, G and B values) is saved as “seattle.smx” in the “matrices” directory.

Three-phase Direct Sky Description Matrix:

The direct sky description matrix is generated by passing the (-d) option in the gendaymtx call and saved as "seattle_direct.smx" in the "matrices" directory. With the exception of the three Tregenza sky patches representing the sun per point in time, the remaining 143 patches (142 sky patches + 1 ground) have an R, G and B value of 0.

High-resolution Sky Description Matrix:

Two additional options are provided to the gendaymtx call for the high-resolution sky matrix: i) the (-5) option refers to the Five-phase method so that only sun positions are included in the output file instead of the entire subdivided sky dome. The argument passed to this option is set as 0.53 (-5 0.53) referring to the solid angle of the disk of the sun. ii) the (-m) option, with the argument of 6 (-m 6), refers to the Reinhart's sky model with 5185 subdivisions to be enforced instead of the

default Tregenza's subdivision model. The output sky matrix description is saved as "seattle_direct_m6.smx" in the "matrices" directory.

3.5 Matrix Multiplication Process:

The Radiance "dctimestep" program is used to multiply the view, transmission, daylight and sky contribution matrices. Since the sky description matrix is created based on the year-round hourly weather data, the outcome of the dctimestep is 8760 luminance distribution maps in the format of a 1000 pixel by 1000 pixel HDR image. In addition, considering the sky matrix is generated as binary float (instead of the default ASCII format), the (-if) option is passed to the dctimestep call so that a binary float input from the sky matrix is expected. As a result, hourly prediction of luminance distribution maps (based on the Three-phase method) is saved in a project folder's sub-directory names as "hourlypics".

A similar `dctimestep` call is made for the multiplication of matrices relative to the Three-phase direct daylight and high-resolution solar components. The outcome of these two `dctimestep` calls is saved, respectively, in the “hourlypics_dir” and “hourlypics_ds” directories.

Chapter 4
Simulation Results

4.1 Annual time-series luminance distribution maps

According to the Five-phase method's equation, the direct daylight component is subtracted from the output of Three-phase simulation results and replaced with the high-resolution direct solar contributions. This process is conducted by a Radiance "pcomb" call where the luminance distribution maps in the "hourlypics", "hourlypics_dir" and "hourlypics_ds" directories correspond with the three parts of the Five-phase equations per point in time. The "pcomb" program allows for applying mathematical expressions on the R, G and B values for every pixel in a luminance distribution map: for each pixel at the coordinates of (x,y), the R, G and B values of the luminance distribution map, for a given point-in-time, in the Three-phase direct daylight contributions ("hourlypics_dir") are subtracted from their counterparts in the Three-phase luminance distribution map ("hourlypics"). The outcome of this subtraction is added the corresponding

R, G and B values of the high-resolution direct sun luminance distribution map “hourlypics_ds”.

The last part of the pcomb expression is independent from the original Five-phase equation. Instead, it is a project case-specific requirement: the rcontrib calls in the matrix computation processes, ignores the assigned glow material that is applied to the computer screens in the simulation scene. Considering the radiance of this light source is constant at any given point-in-time, it is sufficient to add the corresponding RGB values for every pixel that shows the computer screen in the simulated point of view to the outcome of the described RGB subtraction/addition process: a single luminance distribution image is generated where all object surfaces in the simulation scene is assigned with the “black” modifier with the exception of surface polygons for the computer screen. The RGB values for every single pixel in the consequent luminance distribution map, therefore, is equal to 0 except for the RGB values of the pixels representing the computer screen. This computer screen luminance distribution

map is also passed to the pcomb call. The last part of the pcomb expression, therefore, is the addition of the RGB values for a give pixel in the computer screen luminance distribution map to the outcome of the preceding RGB addition/subtraction process.

The final simulation results generated by the pcomb call is saved in a directory named as “hourlyresults” in the project folder. (Figures 20-25)

4.2 The computational processing times

The total simulation time for all described computational processes conducted on a Macbook Pro computer (Processor: 2.5 GHz Intel Core i7, Memory: 16 GB 1600 MHz DDR3) is measured as 196 hours (excluding the genBSDF call for computation of BSDF properties). The simulation of high-resolution direct solar contributions assimilated 122 hours of the total simulation time. The View Matrix and Direct View Matrix simulations are identified as the second and third most time-consuming simulation procedures

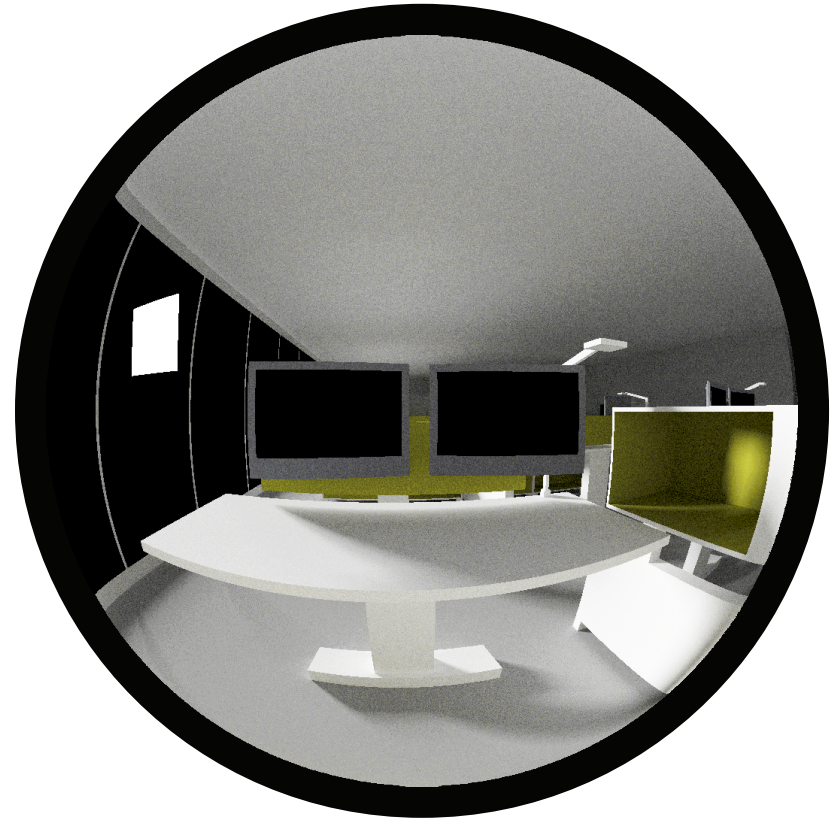


Figure 20: Sample of a View Matrix image relating a single Klems' transmission patch per pixel at the viewpoint

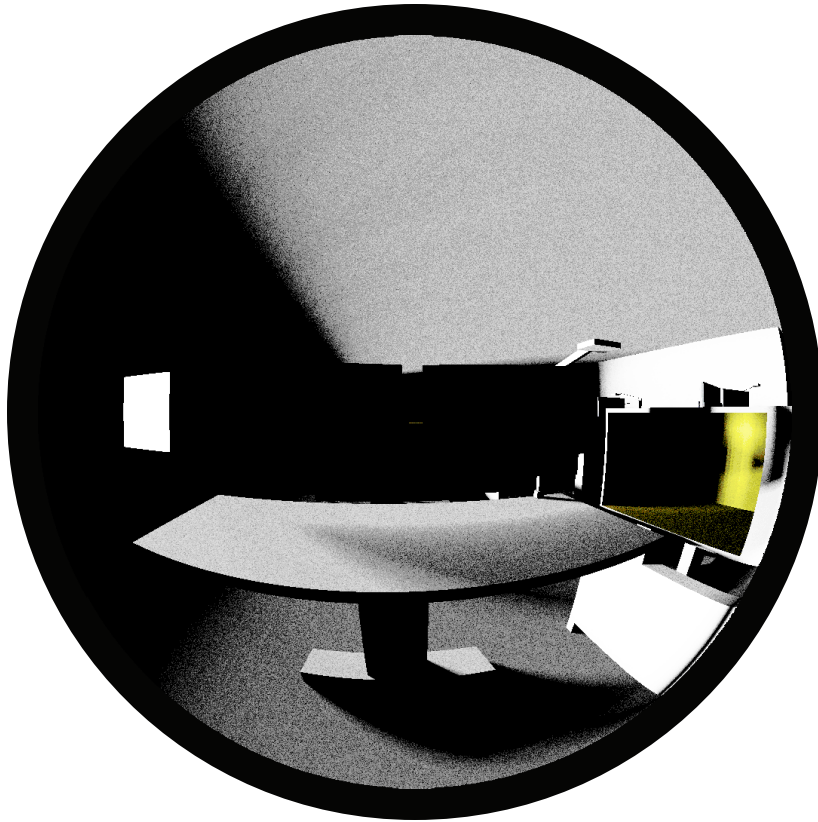


Figure 21: Sample of a Direct View Matrix image relating a single Klems' transmission patch per pixel at the viewpoint

assimilating 28 and 16 hours, respectively, of the total simulation time.

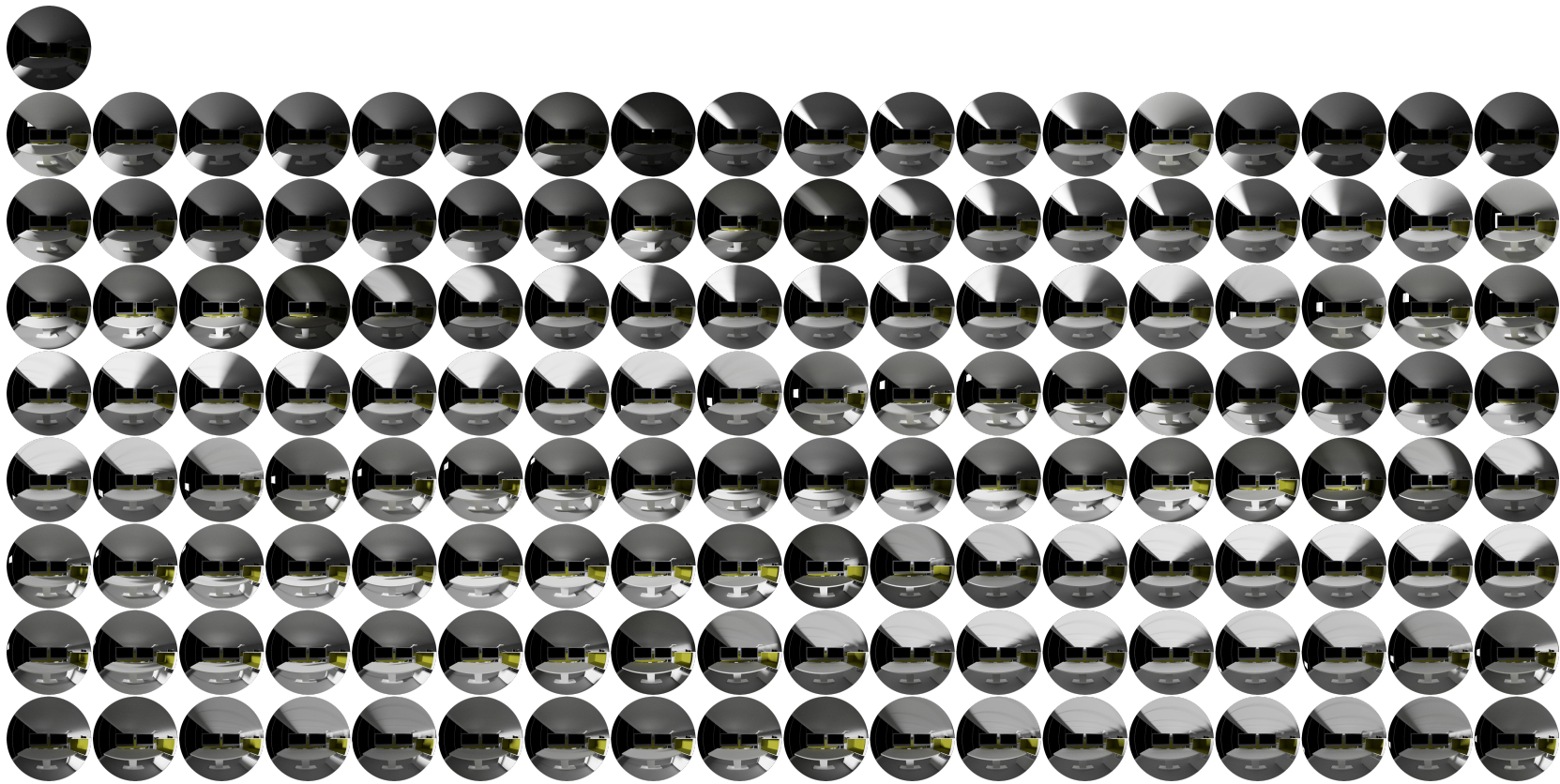


Figure 22: Simulation results for all 145 View Matrix images at the examined occupant point of view

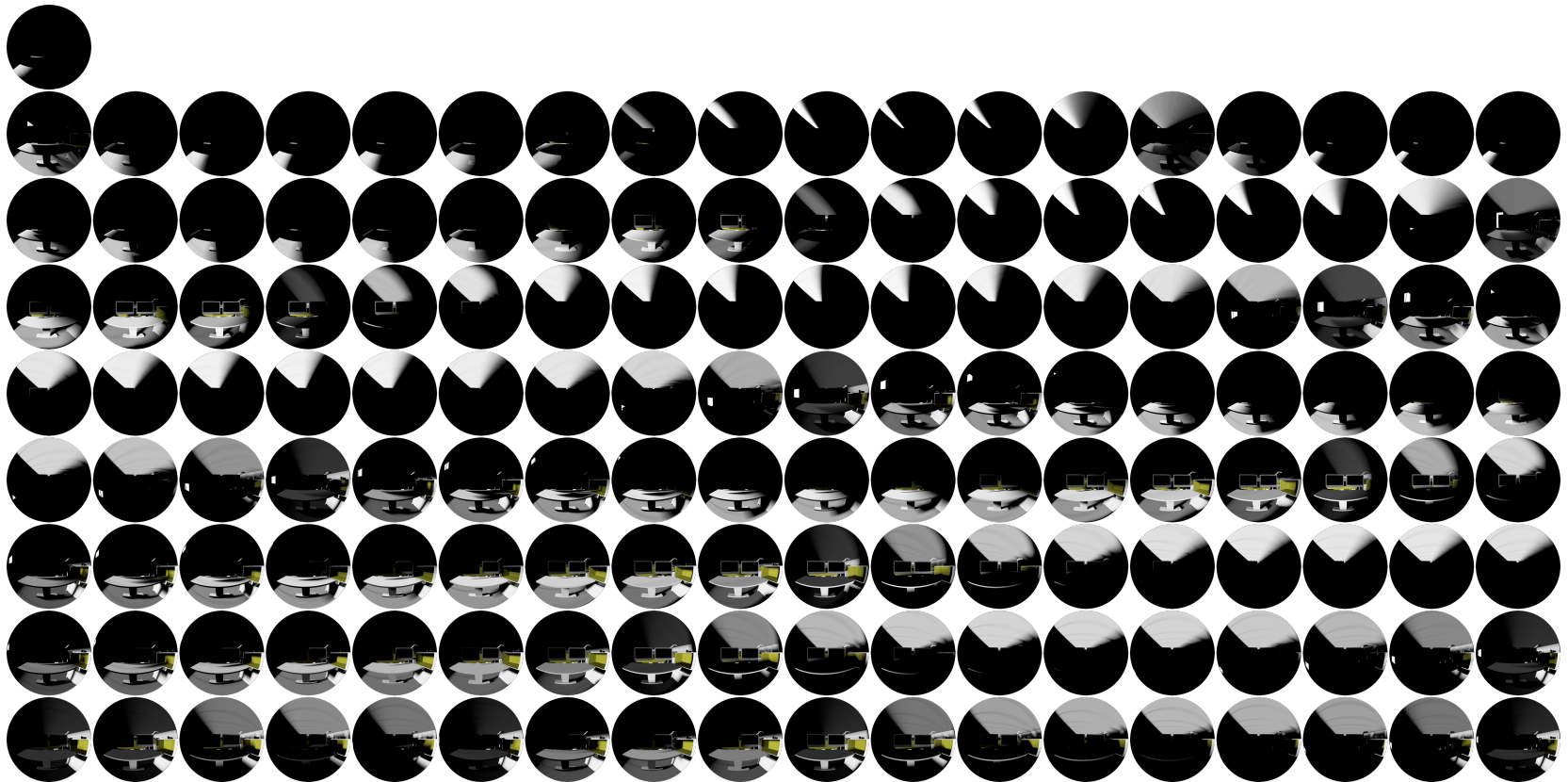


Figure 23: Simulation results for all 145 Direct View Matrix images at the examined occupant point of view

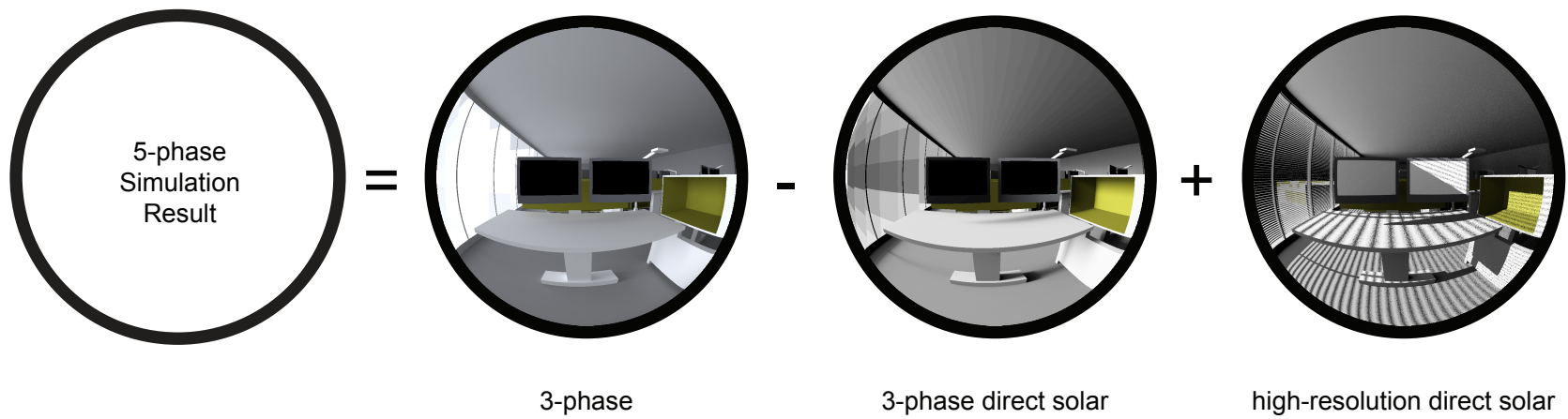
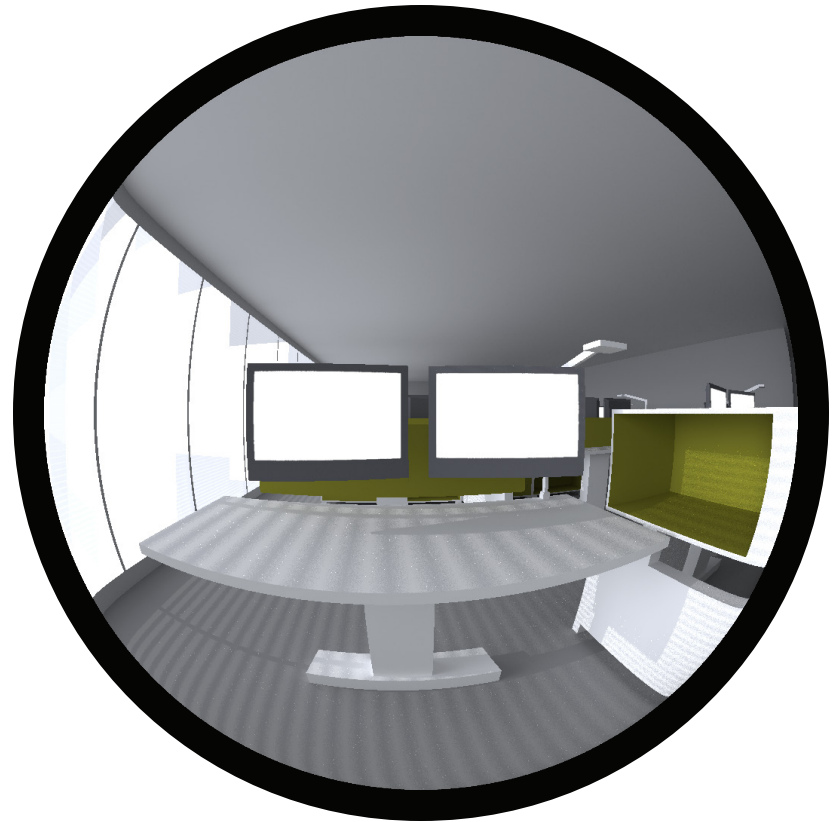


Figure 24: Samples of simulation results for the Three-phase, Three-phase direct solar contributions and the high-resolution direct solar contributions on a single point-in-time (January 1st - 1:00 PM)

Figure 25: Sample of the Five-phase simulation results for prediction of annual time-series luminance distribution at the examiend occupent point of view. (January 1st - 1:00 PM)



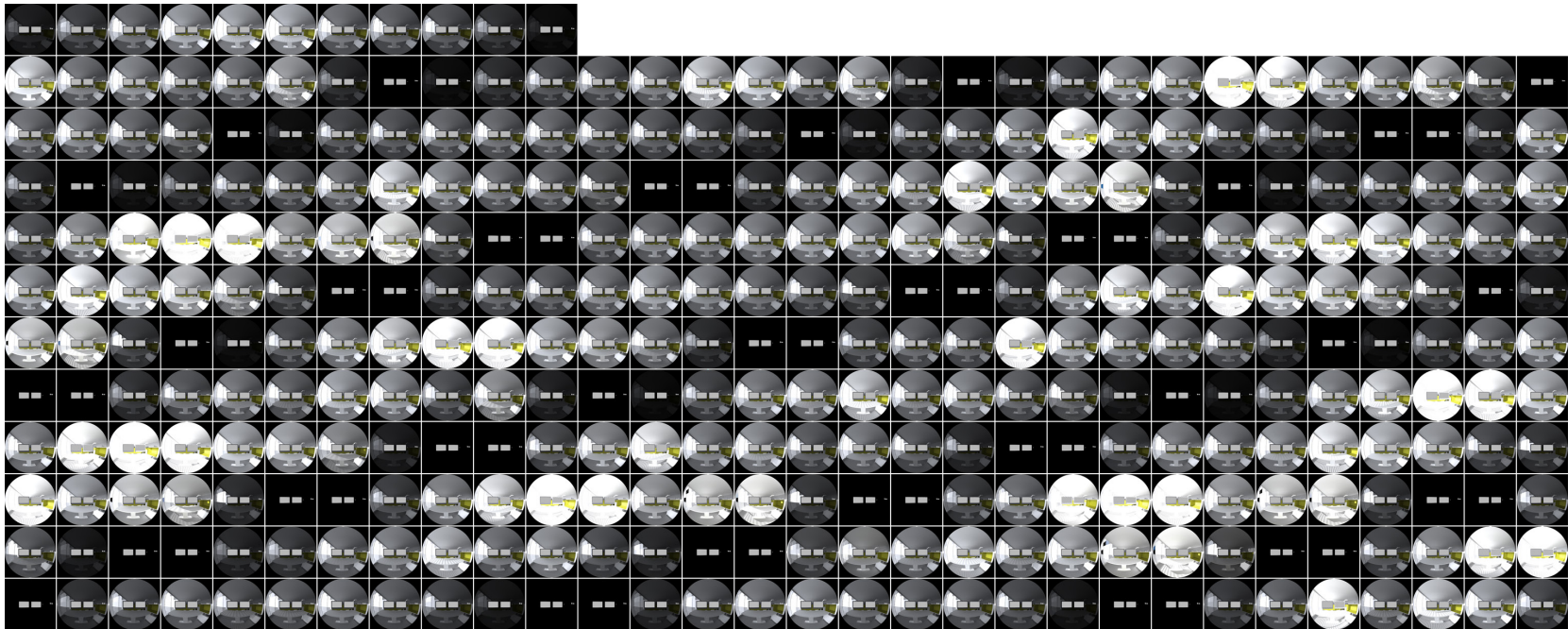


Figure 24: Samples of the Five-phase simulation results for prediction of lumiance distribution maps on a point-in-time basis. (January 08:00 AM - 06:00 PM)

Chapter 5
Conclusions

Conclusions

In this thesis, existing climate-based annual daylight simulation methodologies used for the prediction of point-in-time luminance distribution maps are studied. Computational models that describe each methodology's approach to simulate the luminous flux transfer from the sky dome to a given daylit interior space are illustrated in an office setting. The primary advantages of these simulation methodologies are listed here and discussed as follows: i) their increased capabilities to predict complex simulation scenes, ii) decreased computational processing time and iii) the improvement of the precision of simulation outcome:

5.1 Improved accuracy in the prediction of luminance distribution maps

With the presence of a complex fenestration system in the simulation scene, the outcome of a Three-phase simulation benefits higher accuracy in the predicted

per-pixel luminance value in comparison with the classic Daylight Coefficient methodology. The Three-phase method is advantageous to point-in-time Radiance simulation as it makes it feasible to perform long term simulations. It is also important to note that while the classic Radiance simulation can account for the ray-scattering behavior of the fenestration assembly layers with non-complex geometry (such as the glazing panes), the ray-tracing process with an average number of ambient bounces in a classic Radiance simulation is not sufficient to account for the ray-scattering behavior of fenestration assembly layers with more complex geometry such as venetian blinds. Expanding the comparative evaluation scope in relation to the accuracy of simulation results from single point-in-time to time-series predictions, the daylight coefficient method is analogous to classic Radiance simulation runs given the shared incapability to account for the ray scattering behavior by complex fenestration systems.

The per-pixel luminance calculations from a Five-phase simulation provides a higher precision prediction in comparison with the Three-phase simulation results due to the Five-phase method's capability to account for the direct solar contributions.

5.2 Enhanced comparative evaluation of distinct fenestration systems

The subdivision of the path relative to a luminous flux transfer from the sky to a daylit interior space into three fundamental components as daylight, transmission and view matrices allows for an enhanced comparative evaluation of different fenestration assemblies. Using the Three-phase/Five-phase methods, it is possible to compare the variations in the daylight distribution at a given interior space as a function of the BSDF data relative to different fenestration systems: once the daylight and view matrices are calculated in the first simulation run, the comparison between the daylight distribution impact by two fenestrations systems can be conducted by simply replacing the transmission matrix

according to the respective BSDF data sets. The matrix multiplication, as an arithmetic process, requires significantly less computational processing time in comparison to repetitive simulation procedures for each application instance of a distinct fenestration system in the scene. Such matrix multiplication process also allows for customizing individual assembly layers in a single fenestration system and rapidly access the respective simulation results by each iteration of BSDF data (transmission matrices) per assembly layer.

5.3 Reduced computational processing time

The issue of extensive computational processing time, as a major impediment in time-series simulations using classic Radiance, is addressed by the precedent annual daylight simulation methodologies including the daylight coefficient, Three-phase and the Five-phase methods. The estimated processing time for a year-round time-series Five-phase simulation resulting

illuminance predictions at a target sensor point, in comparison with the prediction of luminance distribution maps at a target point of view, shows a significant margin of difference: given the additional complexities associated with simulation procedures for luminance distribution maps, the typical computational processing time for time-series luminance distribution predictions is disproportionately greater than time-series illuminance predictions. As a result, expanding the hardware-platform for such simulations from a single workstation unit to multiple workstation units or cloud processing servers can transform the annual luminance map predictions to a more accessible data set (just like illuminance predictions) for advanced luminance based daylight analyses.

5.4 Future Developments

While an explanatory guideline based on existing literature of simulation workflows is provided for non-developer designers and daylight practitioners, future development of digital simulation platforms utilizing a graphic user interface is identified as crucial in order to broaden the access to the robust capabilities of the Three-phase/Five-phase methods for a larger group of researchers and practitioners in the area of high-performance building design and sustainability.

The capability of generating simulation-based time-series luminance distribution maps provides an unrepresented opportunity to expand the scope of occupant visual comfort evaluations from a limited number of point of views to a comprehensive set of occupant viewpoints at daylit interior spaces. Such vast data set can be referenced for development of an occupant-centric shading strategy based on a distributed sensing approach using the GlareShade

method. Finally, the availability of data sets for time-series luminance distribution maps relative to a number of examined occupant viewpoints provides a great opportunity for development of new daylight simulation metrics based on cumulative analysis of point-in-time predictions to identify dominant luminance distribution patterns per occupant's point of view during a target period of time.

References:

- Appel, Arthur. "Some Techniques for Shading Machine Renderings of Solids." Proceedings of the April 30--May 2, 1968, Spring Joint Computer Conference on - AFIPS '68 (Spring).
- Bourgeois D, Reinhart CF, Ward G, "A Standard Daylight Coefficient Model for Dynamic Daylighting Simulations" Building Research & Information, 2008, 36:1, pp. 68-82
- Goral, Cindy M., Kenneth E. Torrance, Donald P. Greenberg, and Bennett Battaile. "Modeling the Interaction of Light between Diffuse Surfaces." ACM SIGGRAPH Computer Graphics SIGGRAPH Comput. Graph., 1984, 213-22.
- Ibarra D, Reinhart C F, "Daylight factor simulations - 'How close do simulation beginners 'really' get?'" , Proceedings of Building Simulation 2009, Glasgow, July 2009
- Hashemloo A, Inanici M, Meek C. GlareShade: a visual comfort-based approach to occupant-centric shading systems. Journal of Building Performance Simulation [Internet]. Informa UK Limited; 2015 Jul 9;9(4):351–65. Available from: <http://dx.doi.org/10.1080/19401493.2015.1058421>
- Jakubiec A. and C. Reinhart. "DIVA 2.0: Integrating Daylight and Thermal Simulations using Rhinoceros 3D, Daysim, and Energyplus." Presented at International Building Performance Simulation Association (IBPSA) Conference, Sydney, Australia. 2011
- Klems JH. 1994a. A new method for predicting the solar heat gain of complex fenestration systems: I. Overview and derivation of the matrix layer calculation. ASHRAE Transactions 100 (1): 1065-1072.
- Klems JH. 1994b. A new method for predicting the solar heat gain of complex fenestration systems: II. Detailed description of the matrix layer calculation. ASHRAE Transactions 100 (1): 1073-1086.
- Lawrence Berkeley National Laboratory Window software <https://windows.lbl.gov/software/window/window.html>

McNeil, A. "The Three-Phase Method for Simulating Complex Fenestration with Radiance." Lawrence Berkley National Laboratory (2013).

McNeil, A. "The Five-Phase Method for Simulating Complex Fenestration with Radiance." Lawrence Berkeley National Laboratory, Berkeley, CA, USA (2013).

McNeil, A. & Lee, E.S., 2013. A validation of the Radiance three-phase simulation method for modelling annual daylight performance of optically complex fenestration systems. *Journal of Building Performance Simulation*, 6(1), pp.24–37. Available at: <http://dx.doi.org/10.1080/19401493.2012.671852>.

McNeil, Andrew. On the sensitivity of daylight simulations to the resolution of the hemispherical basis used to define bidirectional scattering distribution functions. DOE Technical Memo, 2011.

McNeil, A., C.J. Jonsson, D. Appelfeld, G. Ward, and E.S. Lee. "A Validation of a Ray-Tracing Tool Used to Generate Bi-Directional Scattering Distribution Functions for Complex Fenestration Systems." *Solar Energy* 98 (December 2013): 404–414. doi:10.1016/j.solener.2013.09.032.

McNeil, A. "genBSDF Tutorial" Lawrence Berkley National Laboratory, CA, USA (2015)
Available at: https://www.radiance-online.org/learning/tutorials/Tutorial-genBSDF_v1.0.1.pdf

Mardaljevic, J. 1995. "Validation of a Lighting Simulation Program Under Real Sky Conditions." *Lighting Research and Technology* 27 (4): 181–188.

Mardaljevic, J. "Daylight simulations: validation, sky models and daylight coefficients", PhD thesis, De Montfort University, Leicester. 2000

Reinhart, C.F. "Daylight availability and manual lighting control in office buildings: simulation studies and analysis of measurement". PhD thesis, Department of Architecture, Technical University of Karlsruhe, Karlsruhe. 2001

Reinhart, C.F. and Walkenhorst, O. "Dynamic RADIANCE based daylight simulations for a full-scale test office with outer venetian blinds" *Energy and Buildings*, 2001, 33(7), 683–697.

Reinhart, C.F. and Andersen, M. "Development and validation of a Radiance model for a translucent panel" *Energy and Buildings*, 2006, 38(7), 890–904.

Reinhart, C.F. "Daysim", Institute for Research in Construction, National Research in Construction, 2001
<http://daysim.ning.com/>

Saxena M, Ward G, Perry T, Hescong L, Higa R. 2010. Dynamic Radiance – Predicting annual daylighting with variable fenestration optics using BSDFs. *Proceedings of SimBuild 2010. 4th National Conference of IBPSA-USA. 2010 August 11-13. New York.*

Tregenza, P.R. and Waters, I.M. "Daylight coefficients". *Lighting Research and Technology*, 1983, 15(2), 65–71.

Tregenza, P.R. "Subdivision of the sky hemisphere for luminance measurements", *Lighting Research and Technology*, 1987, 19, 13–14.

Tsangrassoulis, A. and Santamouris, M.J. "Daylighting modelling with Passport-Light", in *Proceedings of the 5th IBPSA Conference, Prague, Czech Republic, 1997*, pp. 73–78.

Wienold J. and J. Christoffersen. "Evaluation methods and development of a new glare prediction model for daylight environments with the use of CCD cameras." *Energy and Buildings*, 2006, 38: 743-757.

Wienold, Jan. "Dynamic daylight glare evaluation." In *Proceedings of Building Simulation*, pp. 944-951. 2009.

Whitted, Turner. "An Improved Illumination Model for Shaded Display." *ACM SIGGRAPH Computer Graphics SIGGRAPH Comput. Graph.*, 1979, 14.

Ward G, Mistrick R, Lee ES, McNeil A, Jonsson J. Simulating the Daylight Performance of Complex Fenestration Systems Using Bidirectional Scattering Distribution Functions within Radiance. LEUKOS [Internet]. Informa UK Limited; 2011 Apr;7(4):241–61. Available from: <http://dx.doi.org/10.1080/15502724.2011.10732150>

Ward, G. 1994. "The Radiance Lighting Simulation and Rendering System." ACM SIGGRAPH proceedings of the 21th annual conference on computer graphics and interactive techniques, Orlando, 459–472. New York, NY: ACM Press.

Ward, G., and R. Shakespeare. 1997. "Rendering with Radiance. San Francisco", CA: Morgan Kaufman.